Universidade de Aveiro Departamento de Electrónica, Telecomunicações e Informática,
2018

Patrícia Alexandra Pereira Bouça

Agregados de Antenas para Sistemas Massive MIMO 5G e Satélite
Antenna Arrays for Massive MIMO 5G and Satellite Systems

Patrícia Alexandra Pereira Bouça

Agregados de Antenas para Sistemas Massive MIMO 5G e Satélite
Antenna Arrays for Massive MIMO 5G and Satellite Systems

Dissertação apresentada à Universidade de Aveiro para cumprimento dos requisitos necessários à obtenção do grau de Mestre em Engenharia Eletrónica e de Telecomunicações, realizada sob a orientação científica do Professor Doutor Nuno Borges de Carvalho, do Departamento de Eletrónica, Telecomunicações e Informática da Universidade de Aveiro e a co-orientação do Professor Doutor Pedro Pinho, do Instituto Superior de Engenharia de Lisboa.

Dissertation presented to the University of Aveiro for the fulfilment of the requisites necessary to obtain the degree of Master in Electronics and Telecommunication Engineering, developed under the scientific guidance of Professor Nuno Borges de Carvalho, in the Department of Electronics, Telecommunications and Informatics of the University of Aveiro and co-orientation of Professor Pedro Pinho, in High Institute of Engineering of Lisbon.

O júri / The jury

presidente / president

Professor Doutor Telmo Reis Cunha
Professor Auxiliar no Departamento de Eletrónica, Telecomunicações e Informática da Universidade de Aveiro

vogais / examiners committee

Professor Doutor Nuno Borges de Carvalho
Professor Catedrático no Departamento de Eletrónica, Telecomunicações e Informática da Universidade de Aveiro (orientador)

Professor Doutor Rafael Caldeirinha
Professor Coordenador do grupo de Propagação e Antenas- Lr, Instituto de Telecomunicações (arguente)

Agradecimentos

Em primeiro lugar um agradecimento a toda a minha familia pelo incentivo e ajuda ao longo de todo o meu percurso académico e um muito especial ao Bruno por ser meu irmão.

Seguidamente, desejo exprimir os meus agradecimentos a todos aqueles que permitiram que esta dissertação se concretizasse, sobretudo ao Professor Nuno Borges de Carvalho que não poupou esforços para que o trabalho corresse da melhor forma acreditando sempre em mim e nas minhas capacidades e ao Paulo Gonçalves pelo excepcional trabalho com todo o hardware desenvolvido não só para mim mas para todos os colegas.

Ao Manel que foi a pessoa que mais me apoiou nos dias mais complicados e ajudou a ultrapassar todas as dificuldades. Aos meus amigos Cascas, Lourinho, Figas, Sam, Jomi, Jesus, Pika, Tiago, Claudino, Ciclista, Pedro e Rui um enorme obrigado por tudo.

Por fim, os não menos importantes Gwen, Lady, Duke e Kaiser pois nada seria possível sem aqueles que são os melhores amigos do mundo. Uma total dedicatória deste trabalho vai para quem mais o condicionou devido à sua ausência prematura no ano que passou, Kinha.

Resumo

Os sistemas de telecomunicações sem fios continuam a crescer e a melhorar a um ritmo frenético, por isso, novos requisitos têm de ser cumpridos com modificações ao nível do hardware.

A quinta geração exigirá uma revolução, uma vez que as antenas serão projetadas para alta frequência, banda de ondas milimétricas, onde o espetro ainda não foi muito explorado. No entanto, estas frequências são absorvidas com facilidade como, por exemplo, na atmosfera devido à atenuação originada pela chuva. Para resolver estas limitações, os agregados de antenas têm sido estudados devido à sua versatilidade.

Esta dissertação tem o objetivo de desenhar e testar várias soluções baseadas em antenas microstrip (patch). Inicialmente, é realizada uma avaliação do acoplamento entre elementos e propostas algumas técnicas de redução do mesmo, utilizando espaços mais compactos que o usual, mas prevenindo quaisquer diminuições de ganho. Por fim, tendo em vista a mesma limitação espacial, são desenvolvidos agregados de antenas em série direcionados para comunicações via satélite e apresentado um estudo detalhado de antenas para transmissão e recepção em simultâneo.

Abstract

Wireless telecommunications systems are growing and improving at a breakneck pace, and its demands must be fulfilled with hardware modifications.

The fifth-generation will demand a revolution since antennas are going to be designed for high frequency, millimeter wave bands, where there is a lot of unexploited spectrum worldwide. However, these frequencies get absorbed quite easily, for example, they suffer high attenuation due to rain. This implies a decrease of radiated power. To solve some of the issues, antenna arrays have been studied due to their high versatility.

This dissertation has the goal of designing and testing several solutions based on microstrip patch antennas. Initially, an analysis of the coupling between elements is performed as well as some proposed techniques to reduce it, through more compact spaces, without any gain decreasing. Finally, considering the space limitations, series antenna arrays are developed for satellite communications and presented an in-depth study of antennas efficiently employed for both transmission and reception simultaneously.

Contents

List of Figures

List of Tables

Acronyms

5G	fifth Generation
AR	Axial Ratio
IoT	Internet of Things
LNA	Low Noise Amplifier
MIMO	Multiple Input Multiple Output
MMIC	Monolithic Microwave Integrated Circuit
mMIMO	massive MIMO
mmw	milimiter wave
PA	Power Amplifier
RF	Radio Frequency
S-parameters	Scattering parameters
SAR	Synthetic-Aperture Radar
SATCOM	SATellite COMmunications
SMA	SubMiniature version A

Chapter 1

Introduction

Nowadays, massive MIMO (mMIMO) systems are expected to be one of the pillars of fifth Generation (5G) and wireless communications which are growing in demand for better services and solutions. mMIMO entails multiuser Multiple Input Multiple Output (MIMO) which is a common denomination to characterize the future wireless access. The desired improvements for 5G technologies are widely related to antenna arrays because large active antenna arrays will be served many terminals.

Like any other technology, it is expected to have some enhanced capacity, spectral and energy efficiency by using low cost and low power components. However, the challenges are enormous and to overcome the limitations caused by antenna spatial correlation, mutual coupling, and hardware non-linearities some hardware improvements must be made [1].

For the next-generation wireless networks, the specifications and guidelines are set to be [2]:

1. Data rates in the order of 10 Gb/s for specific scenarios;
2. Data rates of more than 100 Mb/s should be generally available in urban and sub-urban environments;
3. Data rates of, at least, a few Mb/s should be available essentially everywhere, including far-off rural and deep indoor environments;
4. Latencies on the order of 1 ms or less;
5. Frequencies of operation above 6 GHz;
6. Wireless devices should operate with extremely low energy consumption and be low-cost.

In the future, 5G technologies should support a great diversity of services in every area. The moment to force mMIMO in 5G has arrived, not just because the current technology cannot deliver the required spectral efficiency, but also because of the reliable, efficient and with low-complexity Radio Frequency (RF) technologies.

1.1 Motivations

The exponential increase in wireless data traffic and the desire to provide services at rates up to Gb/s are leading to a vast amount of research in milimiter wave (mmw) communications, as they become more and more attractive for 5G mobile communication systems, since such rates are not possible in microwave bands. Although this scenario seems to be worthwhile, there are several issues such as the free-space path loss, which is increased by 3 dB when the transmission frequency doubles.

As a result, the motivation for designing sophisticated antennas for mmw communication systems is to overcome the attenuation and path loss between the transmitters and the receivers. One of the solutions that may attenuate this problem is the increase in the number of elements in antenna arrays for the same limited space. The described solution generates coupling between antenna elements, so it is presented, simulated and measured some solutions to this problem.

Contrasting with the overall research, the presented decoupling unit is applied between several elements and not just between two elements. With the increase of elements, the complexity of methods to reduce coupling rise, so it seems to be a better option to research about the impact of the techniques for the growth of elements in a small space.

It becomes challenging when all the antenna design problems for 5G communications are considered, hence the overall knowledge has to be employed to a satellite application. The problem was the same as presented above: in a tiny fixed wing of a satellite, it must be implemented an antenna array with the lowest coupling between elements and still fulfill the gain and radiation pattern requirements.

This work does not comprise all of the options of antenna arrays for satellite applications. The aim is to implement a first attempt and study solutions. Regarding the implementation details, further research would be relevant.

1.2 Objectives

This work focuses not only on the design of antenna arrays for mMIMO solutions, but also in the study of some issues that this new technology brings.

When it comes to antenna arrays for mMIMO solutions, a common concern in 5G communications is the large number of antennas per array. Therefore, a reduction of space between elements is necessary and thus a significant increase in coupling [3].

Another dimension where antenna arrays have been making a difference is in Synthetic-Aperture Radar (SAR) applications. In terms of SATellite COMmunications (SATCOM), the antenna arrays are providing more services dedicated to machine-to-machine communications and Internet of Things (IoT). In the future, it is presumed that wireless communications expand the mobile data rates to multi-Gb/s. These improvements would be provided by the microstrip patch antennas and the way they behave in the mm-wave spectrum. mMIMO solutions should have an available bandwidth spectrum at their higher frequencies, comfortably greater than all cellular allocations of today. As a consequence of increasing the RF channel bandwidth, the data capacity is significantly increased, while the latency for digital traffic is considerably reduced.

This work weighs on designing solutions to compensate for the mutual coupling which is, by this time, one of the limitations associated with many elements in a reduced space.

1.3 Structure Overview

This dissertation is divided into four chapters. Chapter two introduces the definitions of the terms and figures of merit used during the document as well as an overview of some of the already employed techniques presented that are an object of study throughout this work.

Chapter three presents the design and implementation of a technique to reduce mutual coupling. It also contains the experimental results achieved with the printed arrays. Chapter four contains the design and some implementation of antenna arrays for SATCOM as well as the lab measurements. There is also a study of the techniques used to achieve circular polarization with a microstrip patch antenna.

The last chapter includes the conclusion of the measured boards when compared with the simulated results and a proposal for future work.

1.4 Contributions

This dissertation work resulted in a paper submission and acceptance in the IMWS-5G 2018 called "Mutual Coupling Reduction Using Grounded Copper Vertical Plane Structure" - P. Bouça, N. B. Carvalho and P. Pinho. The topics addressed and developed were related to the implementation of new decoupling structures for mMIMO applications.

Chapter 2

State of the Art on Antenna Arrays

The concepts introduced in this chapter were crucial to achieving the desired results for the microstrip antenna arrays implementations. Firstly, there is an introduction of all the basic concepts not only related to the patch antenna design but also about the feeding methods. The theoretical notions of a single microstrip patch antenna are taken into consideration when it comes to array designing, so it is critical to study them to choose better which one is the best to opt for specific situations.

Secondly, it is presented a common concern in 5G antenna arrays designs known as mutual coupling. According to the recent literature, the reduction of the area that an array occupies is significant to get the best radiation patterns and gain, using the smallest space possible. However, this reduction profoundly affects the Scattering parameters (S-parameters). This problem is going to be described, and the solutions studied and implemented are going to be presented.

Finally, the microstrip patch antenna series feed arrays are introduced. These arrays are a very good solution because of its limited space and high gain. They also offer a decent disposition when it is desired to have the transmission and reception separated. In connection to Fthis, it is at last presented the circular polarized antennas as a hypothesis to get the transmission in the right and reception in the left polarization.

2.1 Microstrip Antennas

Since microstrip antennas were firstly introduced, they became the most common type of antennas in radio frequency designs. These antennas are composed by a metallic patch on a grounded substrate. There are a lot of configurations that can be used for the metallic patch, but the most common one is the rectangular shape. These radiating elements

present light weight, low profile, conformable to planar and nonplanar surfaces, simple and inexpensive to fabricate using modern printed-circuit technology, mechanically robust when mounted on rigid surfaces, compatible with Monolithic Microwave Integrated Circuit (MMIC) designs, and very versatile regarding resonant frequency, polarization, pattern, and impedance [4].

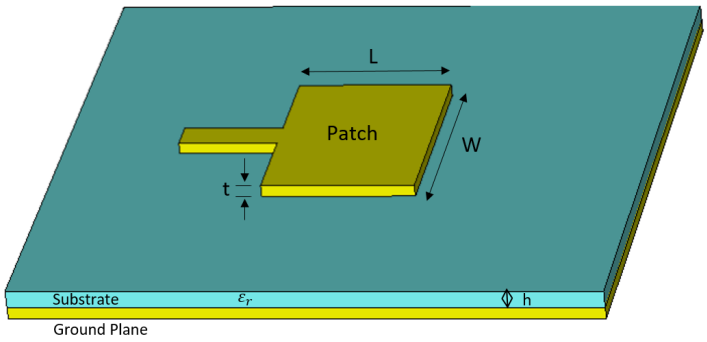

Figure 2.1: Rectangular microstrip (patch) antennas.

A rectangular patch and its dimensions are presented in Figure 2.1. To have a resonant antenna, L should be approximately $\lambda/2$ and W smaller than λ_0. The substrate thickness, h, has a permittivity between 2 and 24. It happens to have two radiating slots separated by a distance L, which corresponds to the fringing fields. As discussed above, the separation $\lambda/2$ causes 180 degrees phase shift. However, if viewed from the top of the antenna, the fields are in phase when considering the x-axis' components, so the broadside radiation has its maximum in the z-axis direction[5]. The fringing fields effects are going to have a contribution to the alteration of the L that is given by

$$\Delta L = \frac{0.412d(\epsilon_{reff} + 0.3)(\frac{W}{d} + 0.264)}{(\epsilon_{reff} + 0.258)(\frac{W}{d} + 0.8)} \tag{2.1}$$

Where the effective relative permittivity is

$$\epsilon_{reff} = \frac{\epsilon_r + 1}{2} + \frac{\epsilon_r - 1}{2}[1 + 12\frac{h}{W}]^{-1/2} \tag{2.2}$$

By solving Equation 2.3 in order to L

$$L = \frac{1}{2f_r\sqrt{\epsilon_0\mu_0}\sqrt{\epsilon_{reff}}} - 2\Delta L \tag{2.3}$$

It is also possible to calculate the width for an efficient radiator, which is given by

$$W = \frac{1}{2f_r\sqrt{\epsilon_0\mu_0}}\sqrt{\frac{2}{\epsilon_r + 1}} \tag{2.4}$$

Where the resonant frequency for TM_{010} mode is given by

$$f_r = \frac{1}{2(L + 2\Delta L)\sqrt{\epsilon_{reff}}\sqrt{\epsilon_0\mu_0}} \tag{2.5}$$

2.1.1 Feeding Techniques of Microstrip Patch Antennas

Microstrip patch antennas may be powered by different feeding methods that can be distinguished by being with or without contact. On one hand, it is possible to connect a feeding line directly into a radiating patch, while on the other hand, it is also possible to achieve a transference of power between a microstrip line and a radiating patch due to the electromagnetic coupling field [6].

The patch antenna can have different feed configurations, including microstrip line feed and aperture coupled [5]. The advantage of having the possibility of using different feeding techniques is that each one presents their own benefits.

A. Line Feeding

Line feeding process consists of directly connecting a microstrip line to the edge of the microstrip antenna. It can either have a transformer and a 50Ω line, Figure 2.2, or only a line. This technique grants the advantage of providing a planar shape, so the width of the conducting element is smaller when compared with the microstrip patch antenna [5].

B. Aperture coupled feed

In aperture coupled feed, Figure 2.3, the microstrip feed line is separated from the patch by a ground plane which is coupled through a slot, usually centered under the patch, in the ground plane. The ground plane slot may have different forms, and its width and length will have a significant impact on the variation of the coupling. Consequently, can improve the result of bandwidth and reflection coefficient [5].

This technique has moderate spurious radiation and polarization purity because of the ground plane between the substrates, which isolates the feed line from the radiating patch and minimizes interference. However, it is the most difficult one to fabricate, and it also has narrow bandwidth [4].

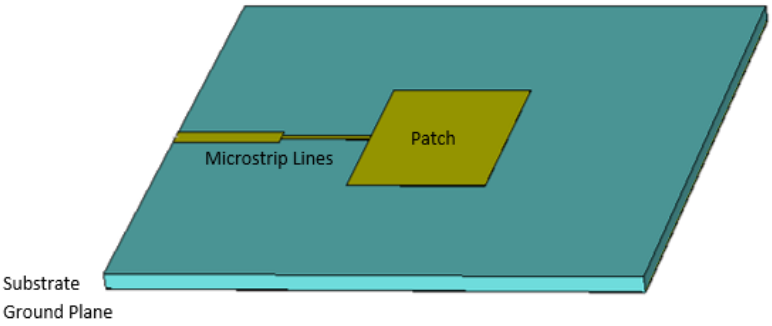

Figure 2.2: Microstrip feed

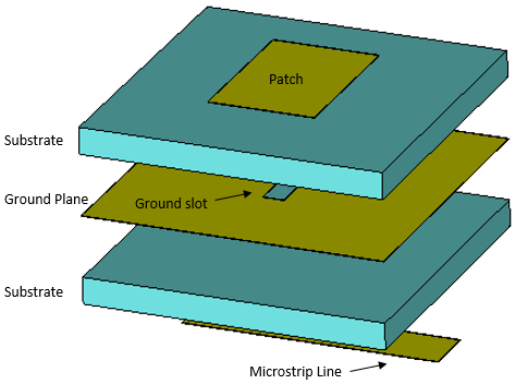

Figure 2.3: Coupling feed

2.2 Antenna Array for 5G applications

Antenna arrays were introduced to solve some of the issues and accomplish some requirements and standards that single-element antennas cannot achieve. These elements are a solution to fulfill the necessities of wireless mobile communications services, to enhance the efficiency of mobile communications systems and to overcome the problem of limited channel bandwidth. An antenna array, Figure 2.4, improves the channel capacity and spectrum efficiency to achieve a better performance in communication systems [7].

A single-element antenna presents limited gain and lack of flexibility when it comes to producing the desired radiation pattern by suitably choosing the phase and amplitude distribution between the elements. It consists of a few antenna elements which are strategically placed to form a structure with specific characteristics. The overall array radiated field is determined by a single vector that is calculated by the vector addition of every element's vector [5], and it can be obtained by

$$E(r,\theta,\phi) = (\sum_{n=1}^{N} E_N)(J_n) \tag{2.6}$$

To achieve specific radiation characteristics, there are a couple of variables to be considered, including the radiation pattern, the number of antenna elements and its excitation as it is shown in Figure 2.4.

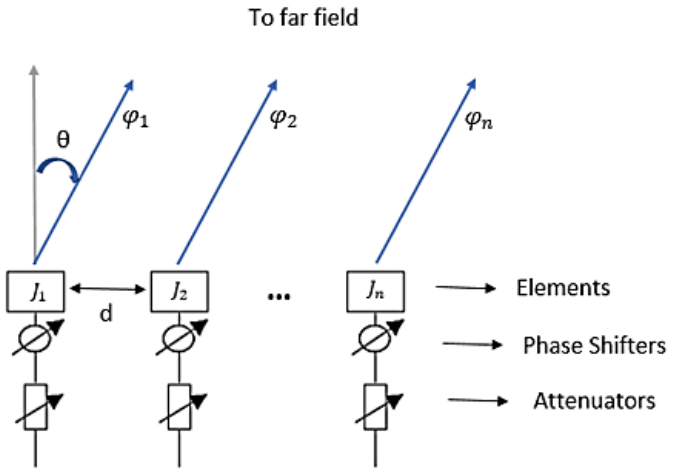

Figure 2.4: Antenna array of N elements

2.3 Mutual Coupling in Antenna Arrays

When two antennas are placed near to each other, they interact if one or both are transmitting or receiving. The energy flowing through one may have a significant impact on the other. This interaction between elements due to their proximity is called mutual coupling [5].

To analyze the mutual coupling between elements, it is defined and used the reflection and transmission coefficients for circuit and field problem examinations where single antennas and antenna arrays are included. There is a general analysis assuming that any of these elements are a two-port network. In Figure 2.5, is illustrated a two-port network that is characterized by the S-parameters.

Figure 2.5: A two-port network

When N=2, the presented case, in which we can consider the existence of two antennas, the matrix that links the output and the input is given by

$$\begin{bmatrix} b_1 \\ b_2 \end{bmatrix} = \begin{bmatrix} s_{11} & s_{12} \\ s_{21} & s_{22} \end{bmatrix} \begin{bmatrix} a_1 \\ a_2 \end{bmatrix}$$

Thus, the S-parameters are

$$\begin{aligned} s_{11} &= \text{Port 1 reflection coefficient} \\ s_{21} &= \text{Port 2 to Port 1 transmission coefficient/gain} \\ s_{12} &= \text{Port 1 to Port 2 transmission coefficient/gain} \\ s_{22} &= \text{Port 2 reflection coefficient} \end{aligned}$$

If the network is passive and loss free, there is a relation of reciprocity which means that $s_{12} = s_{21}$.

The S-parameters are clearly linked to antennas because a transmitting-receiving antenna system is, in fact, a 2-port network. Transmission and reflection can be characterized using S-parameters. The s_{11} and s_{22} parameters indicate how well the antenna feed line is

matched with the antenna itself. The s_{12} and s_{21} parameters are the transmission coefficients between the two antennas [5]. These two parameters are determined by the characteristics of the antennas and the distance between them. They are commonly analyzed to characterize the mutual coupling between elements.

There are several reasons for the interchange of energy between elements, for example, while the two antennas are transmitting, the second one receives some of the energy radiated from the first one, Figure 2.6, due to the directional characteristics being non-ideal. On one hand, the antenna is transmitting, while on the other hand, part of the energy that should be incident is rescattered in different directions that may be difficult to predict analytically [4].

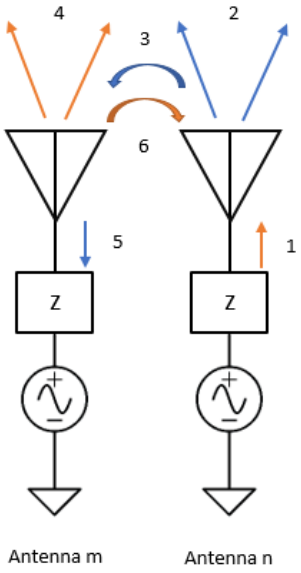

Figure 2.6: Mutual coupling representation for transmitting mode

Mutual coupling depends on the radiation characteristics of each element, the separation between elements and its relative orientation that affects the current distribution, the input impedance and the radiation pattern [5] [4].

An antenna array of N elements is treated as a N-port network, considering each one to be a current source and having an impedance when looking into a single isolated element given by

$$Z_{nn} = \frac{V_n}{I_n} \tag{2.7}$$

where $n = 1, 2, ..., N$.

The impedance Z_{mn}, called the mutual impedance, occurs due to the proximity of the m and n antennas, Figure 2.6, and is given by

$$Z_{mn} = \frac{V_m}{I_n} \tag{2.8}$$

The biggest concern, for example in [8], is that mutual coupling is mainly dependent on the distance between the closest elements in an antenna array, so the resonant frequency, bandwidth, and match performance are not spoiled for spacing greater than $0.4\lambda - 0.5\lambda$. It is also considered that for a shorter distance, the mutual coupling can result in antenna mismatching, side-lobe level increase, and antenna array gain decrease.

For decreasing mutual coupling, it is considered the benefits of using a slotted ground plane structure. In [9], there is a description of how the number of slots can influence the amount of energy filtered through themselves. Commonly, it has been discussed the mutual coupling between two patch antennas [10][11]. However, few works took into account how highly the coupling can increase when considering more elements.

2.4 Antenna Arrays for SAR applications

SAR systems antenna arrays have a lead role in determining the overall system performance because of its major impact on systems' sensitivity, spatial resolution in both range and azimuth, image ambiguities, and swath coverage. The majority of these aspects are primarily influenced by the beam forming and beam scanning capability of the antenna. Recently, through many studies, such as in [12], a massive inclination to use circular polarization in the antenna arrays has been pointed out. In [13], the interest of adding two frequencies dually polarized is explained. A singly polarized frequency provides a monochromatic image. The frequency also has a crucial role since the higher ones offer a better image quality.

A niche market is emerging to rapidly perform low-cost missions on very small spacecrafts, commonly known as CubeSats, Figure 2.7. Their potential has been widely increasing for a variety of applications, such as data communication system where the antenna is growing in importance.

The microstrip patch antennas are being developed using two approaches: transparent antennas that go above the solar panels [14] and non-transparent antennas that go below the solar panels [15]. Transparent conductors may be applied to design transparent antennas, but they have lack of efficiency at S-band frequencies. A favorable solution for the

Figure 2.7: A 1U CubeSat with a wire antenna deployed in space - Image courtesy of Montana State University, Space Science and Engineering Laboratory

satellite applications presented was, for example, the usage of meshed patch antennas with a circular polarization [14].

The azimuth and elevation angles (look angles) for the ground station antenna are imperative to track the satellite correctly. The look angles may have to change to track the satellite. The way to do so may be by changing the beam of the antenna or by a mechanical structure. With the geostationary orbit, this problem is not a concern once the satellite is stationary in relation to the earth [13].

As it is possible to conclude, there are many approaches when it comes to design antenna arrays for SAR applications, for example in [16], the goal was to demonstrate the viability of the dual-band and dual-polarized array concept. This concept has been growing on argue for SAR antenna arrays. The main idea is to benefit from the polarization in order to be able to transmit and receive.

2.4.1 Series Feed Antenna Arrays

Series feed can be applied to linear and planar arrays with single or dual polarization. It is based in setting microstrip patches feed in series with microstrip transmission lines connecting their radiating edges, Figure 2.8. Due to its configuration and the placement of the elements, any change in an element or line affects the performance of the others. It may cause a degradation of the return loss, increasing of the mutual coupling and internal reflections in the overall antenna array [4] [17].

One of the advantages of these arrays is that they have a low feeding loss, which makes

them especially effective for the millimeter wave application. However, they commonly have narrow band which is a considerable limitation for some purposes.

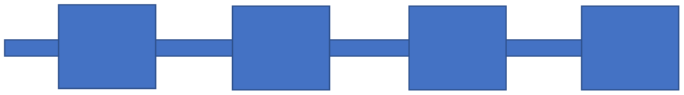

Figure 2.8: Microstrip patch arrays with series feed

It also presents limitations when it comes to the beam direction that is sensitive to frequency, producing a specific amplitude taper [17].

The microstrip patch antennas are separated by a microstrip transmission line which has a $\lambda/2$ length. Theoretically, the characteristic impedance of the transmission lines between elements is not a concern because the loads created by the edges of each element should be $\lambda/2$ in spacing [18].

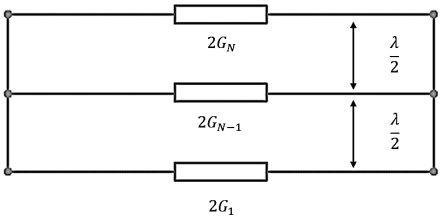

Figure 2.9: Brief representation of microstrip elements as lumped resistive loads

In Figure 2.9, it is presented a microstrip antenna as lumped resistive loads where G_N is the edge conductance at the edge of each patch. The equivalent R_{in} in dependence of G_N and the number of elements, N, is given by

$$R_{in} = (2\sum_{n=1}^{N} G_N)^{-1} \tag{2.9}$$

The first technique discussed presents patches of identical width for a situation where it is considered that the excitation amplitude is the same for all of the elements. Due to this situation, the value of G_N, slot conductance, is always the same. The array side lobes may be decreased by the implementation of another method that consists of changing the widths of the edge of patch antennas, Figure 2.10, so they accept a designated amount of power in order to produce an amplitude taper [17].

Figure 2.10: Microstrip patch arrays with series feed using different widths

This technique implies that the transmission characteristics of each element have to be determined accurately, to achieve a desired amplitude and phase distributions. It also should be taken into account the cumulative transmission characteristics of preceding elements [17] [19].

A certain amount of phase shift error in series feed arrays was noticed. The results in [20] demonstrate the limitations of the simple transmission line model that is often used to analyze series feed arrays and the importance of taking into account the mutual coupling between the elements which are commonly neglected in this type of arrays.

Some works, for example in [21], claim that when an open stub is used, Figure 2.11, the realized gain will be improved by adjusting the stub length since the reflected wave at the end can be utilized. However, the bandwidth is further narrowed. A vertical pattern that is formed by the series feed can be realized by a set of proper patch width and spacing[21].

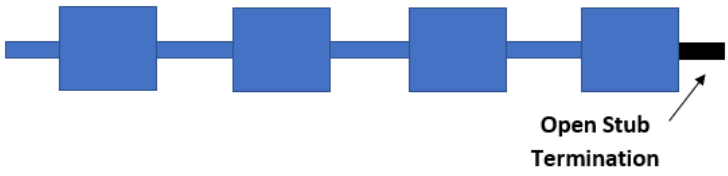

Figure 2.11: Microstrip patch arrays with series feed using open stub termination

2.4.2 Circular Polarization

The polarization depends on how the current flows in the antenna. For circular polarization, two orthogonal currents with 90° phase offset should travel along. The wave propagation towards the z-direction can be expressed using a trigonometric form where, A and B are the amplitudes of the field components in the x and y directions, respectively, Equation 2.10.

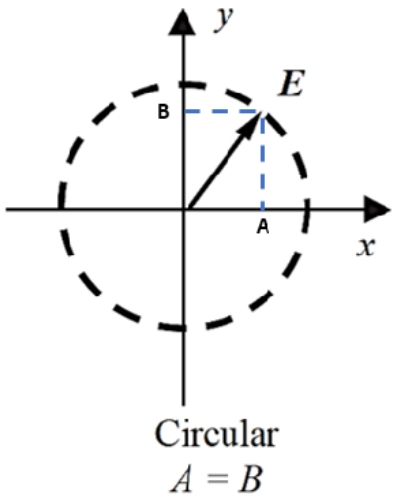

Figure 2.12: Circular wave polarization

If $A = B$, the wave is circularly polarized, Figure 2.12, known by its wide utilization in SATCOM. Independently of the technique used, it is possible to consider that there is circular polarization if two orthogonal modes are excited with a 90° time-phase difference

between each other [4] [5].

$$E = \hat{x}Acos(\omega t - \beta z) + \hat{y}Bsin(\omega t - \beta z) \tag{2.10}$$

A comparison of E_θ, the far-zone electric field radiated by a short dipole, and E_ϕ, electric field radiated, indicates that the two components are in time-phase quadrature, a necessary but not sufficient condition for circular polarization. The Axial Ratio (AR) is given by

$$AR = \frac{A}{B} = \frac{|E_\theta|}{|E_\phi|} \tag{2.11}$$

If AR has a value of 1, it is considered circular polarization. However, the closer it is to 1, the closer it is to circular polarization. In [4], it is precisely said that an antenna is circularly polarized when AR becomes the unity, which corresponds to 0 dB.

Circular polarization may provide some desired extra features for many applications. The microstrip patch elements presented so far radiate primarily linearly polarized waves if conventional feeds are employed with no modifications. There are plenty techniques of feed arrangements, Figures 2.13 and 2.15, or element modifications, Figure 2.16, with which circular and elliptical polarizations can be obtained [4].

A. Single-feed arrangements

For single feed circular polarization antenna design, it may be used a nearly square patch fed at a point along the diagonal line of the patch.

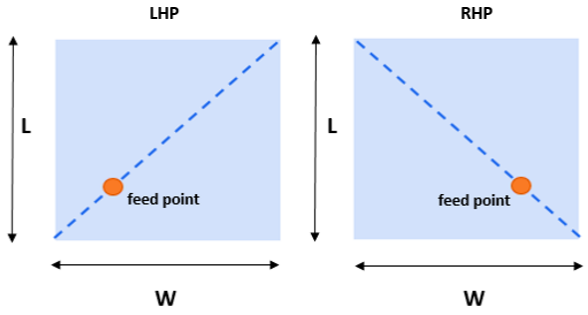

Figure 2.13: Single feed arrangements for circular polarization

B. Quadrature hybrid coupler

Quadrature hybrid coupler is a passive microwave component used for power division or power combining. Hybrid junctions usually have equal power division with either a 90° or a 180° phase shift between the output ports.

One of the proposed ways to make circular polarization is to use the phase shift of 90° between two output ports caused by the symmetric coupler, Figure 2.14.

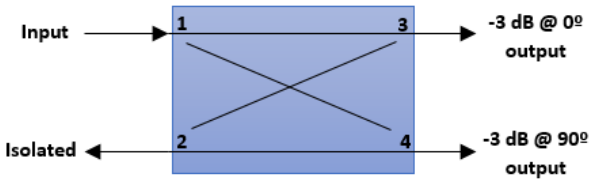

Figure 2.14: Quadrature hybrid coupler

A 90° hybrid junction will ideally lead to a perfect input match at the input port over a wide frequency range, and its phase characteristics lead to an ideal cancellation of reflections at the input port.

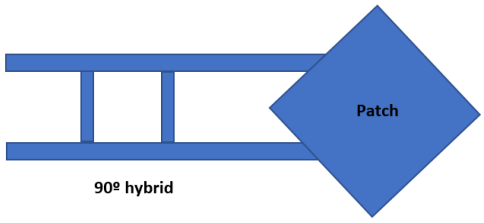

Figure 2.15: Square patch driven at adjacent sides through a 90° hybrid

C. Trimmed square

A square patch antenna with two corners truncated can also introduce circular polarization, Figure 2.16. If the aperture feed is used with a single slot, the feed network will be much simpler when compared to the dual feed circular polarization antenna, Figure 2.15. Circular polarization is realized due to the excitation of two orthogonal modes with a 90° phase shift which happens as a result of perturbations of the trimmed patch.

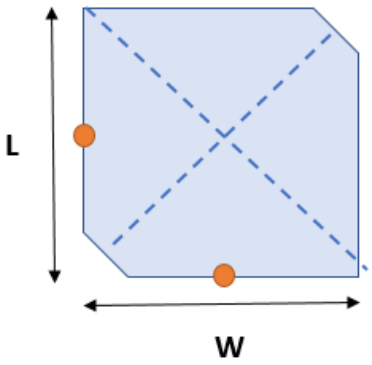

Figure 2.16: Trimmed square (L = W)

Chapter 3

Techniques to reduce the mutual coupling and to improve isolation between antennas

3.1 Conventional 8-element antenna array

In this chapter, it will be discussed the coupling impact in an 8-element microstrip patch antenna array and some new solutions to reduce its mutual coupling. A parametric study was made to determine the influence of mutual coupling depending on the distance between each element.

Usually, the input impedance is designed so it has the desired value, but it can be hard to reduce the coupling between two closely spaced antennas. So, it is presented a study on the impact of the edge to edge spacing of 0.1λ to λ between elements at 5.8 GHz in an 8-element array with good input impedance matching but poor port isolation. A detailed image of the antenna array design and its dimensions are shown in Figure 3.1 and Table 3.1. The antenna array consists of a rectangular aperture coupled feed with a slot located in the ground plane, placed on a 1.52-mm-thick ISOLA Astra substrate (relative permittivity equals 3 at 5.8GHz). The ground plane and the radiating patches are made from copper with $0.035mm$ of thickness, and the slot of each element is excited by a 50Ω microstrip located on the back of the bottom layer, Figure 3.2.

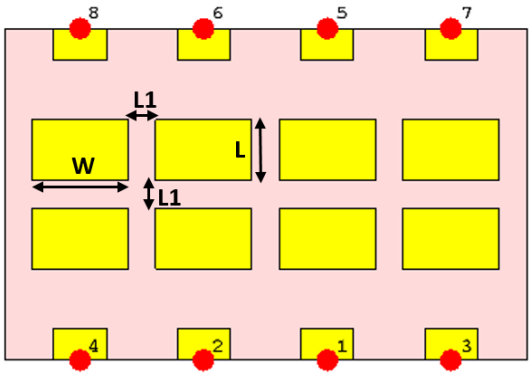

Figure 3.1: Top layer of the 8-element antenna array

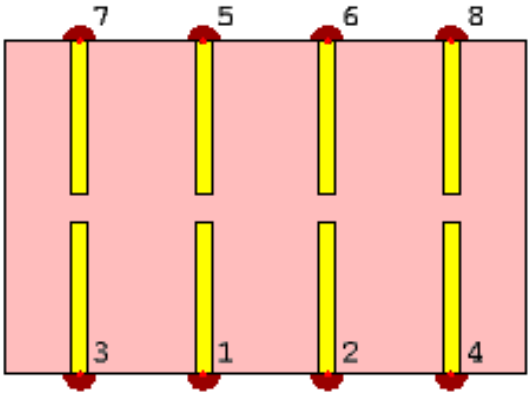

Figure 3.2: Bottom layer of the 8-element antenna array

Symbol	Description	Length (mm)
λ	Wavelength	51.724
L1	Edge to edge distance [0.1λ ; λ]	[5.1724;51.724]
L	Patch length	18.275
W	Patch width	11.55

Table 3.1: 8-element conventional antenna array structure parameters

3.1.1 Simulation Results

The S-parameters of the antenna array are shown in Figures 3.3 and 3.4, regarding the edge to edge spacing between the two closest microstrip patch antennas. The mutual coupling presents the expected variation where the reflection coefficient is below -10dB.

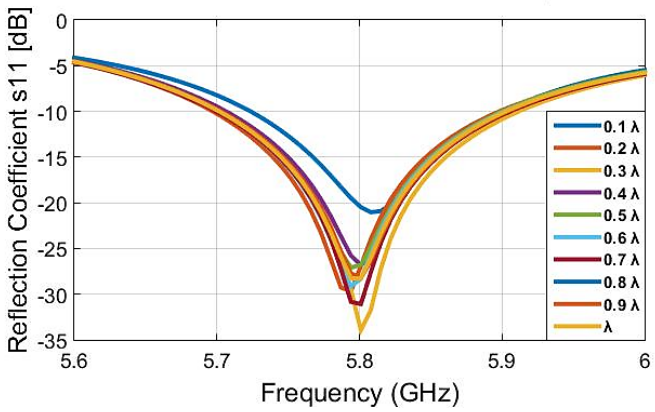

Figure 3.3: Simulated s_{11} of the conventional antenna array of eight elements

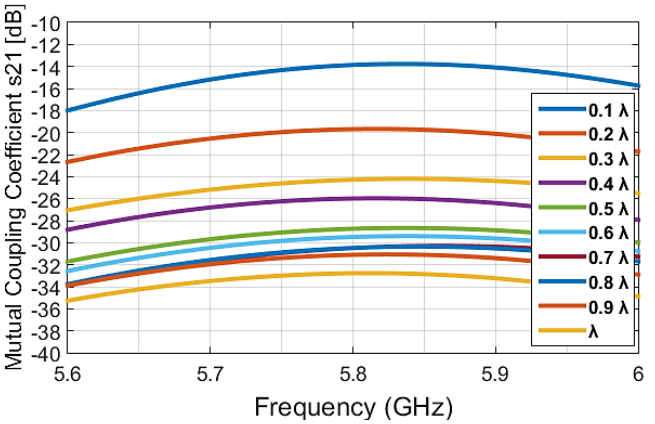

Figure 3.4: Simulated s_{21} of the conventional antenna array of eight elements

Considering the first simulated results, we can conclude that the worst scenario is to place the antennas at the minimum distance, 0.1λ. As a result, this study will be focused on the 0.1λ edge to edge distance between elements.

3.1.2 Measurement Results

In Figure 3.5 is a photography of the 3D printed board of the conventional antenna array.

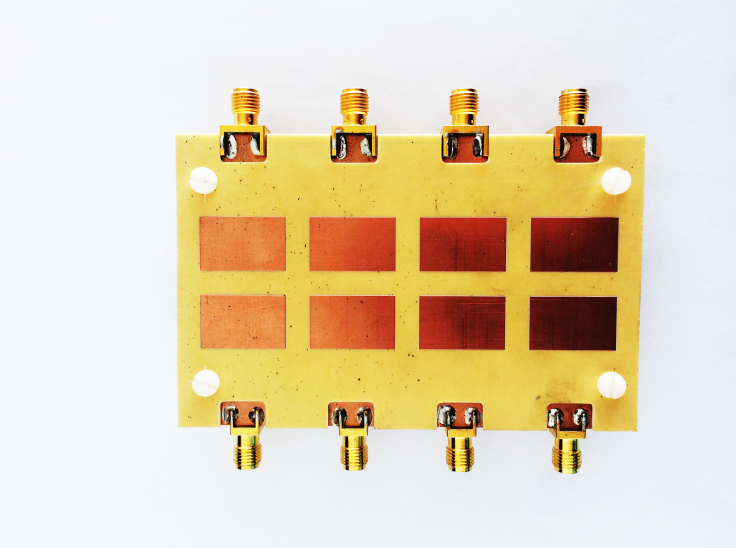

Figure 3.5: Board of the conventional antenna array of eight elements

There was a deterioration of the reflection coefficient parameter that can be explained by the misalignment of the two boards. However, the adaptation was still accomplished, Figure 3.6. The measurement results for mutual coupling were very similar to the simulated ones, Figure 3.7.

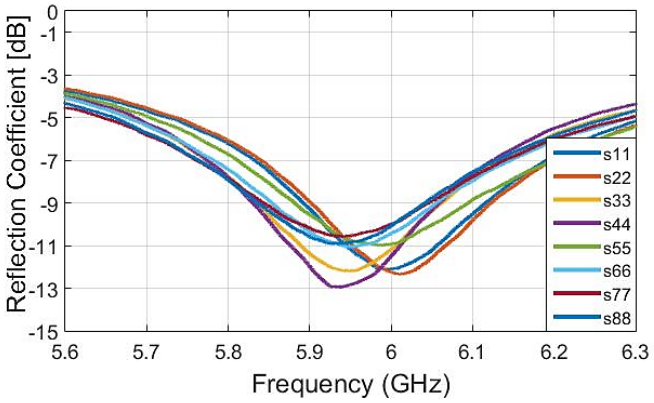

Figure 3.6: Measured reflection coefficient of the conventional antenna array of eight elements

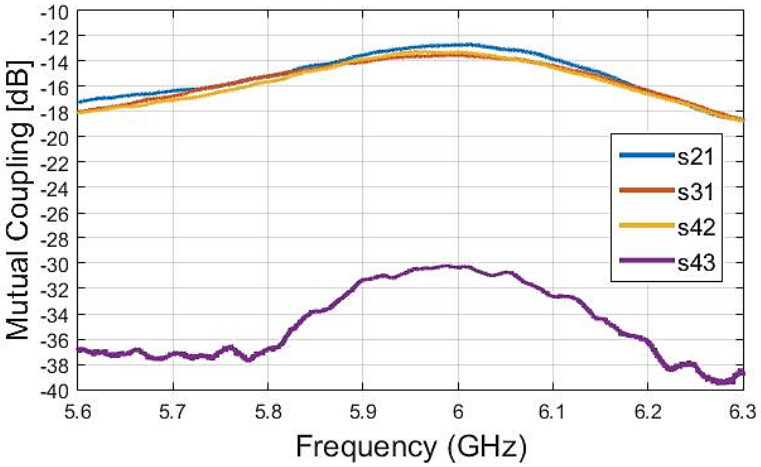

Figure 3.7: Measured coefficients related to mutual coupling of the conventional antenna array of eight elements

3.2 Grounded vias in an 8-element antenna array

The first procedure to reduce mutual coupling for a very small distance between elements, 0.1λ, was the introduction of periodical cylindrical slots considering the edge to edge distance between antennas of 0.1λ. For decreasing mutual coupling, the benefits of using a slotted ground plane structure are considered because these can influence the amount of energy filtered through themselves.

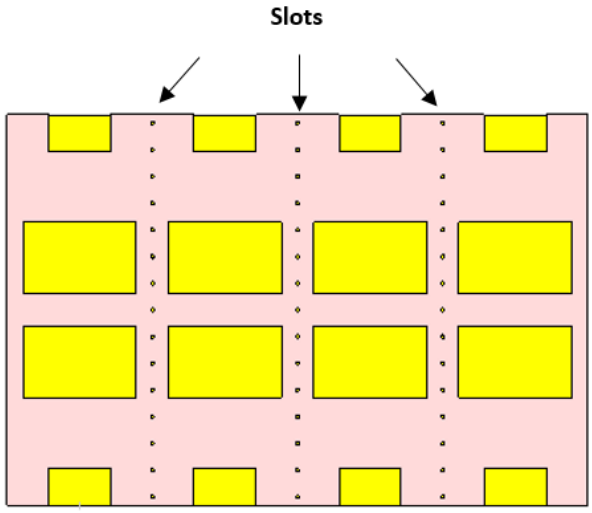

Figure 3.8: Top layer of the 8-element antenna array with the ground slots

The importance of the radiuses of the slots was also studied, varying them from 0.4-0.8 millimeters. It is presented a study on how the mutual coupling behaves with the increasing of the slot radius. The results presented for the reflection loss were satisfying, proving that the addition of the grounded slots do not represent a way to cause deterioration of this parameter, Figure 3.9. A difference of less than 1 dB was achieved for the mutual coupling reduction, Figure 3.10.

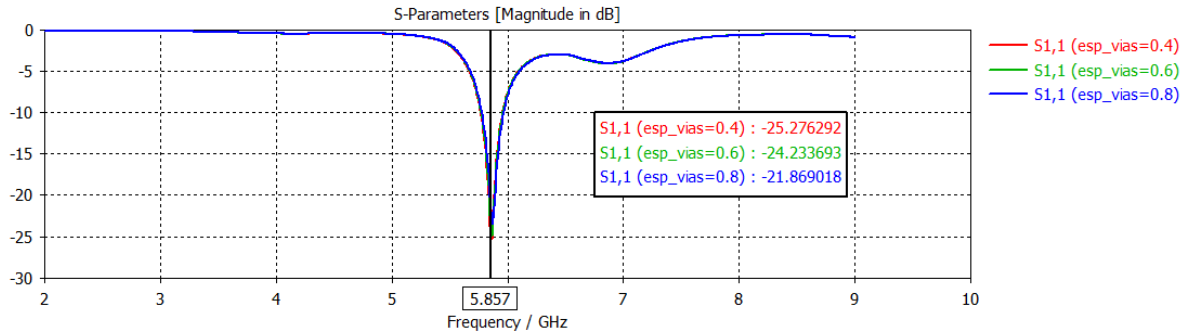

Figure 3.9: Simulated reflection coefficient of the antenna array of eight elements with the grounded vias

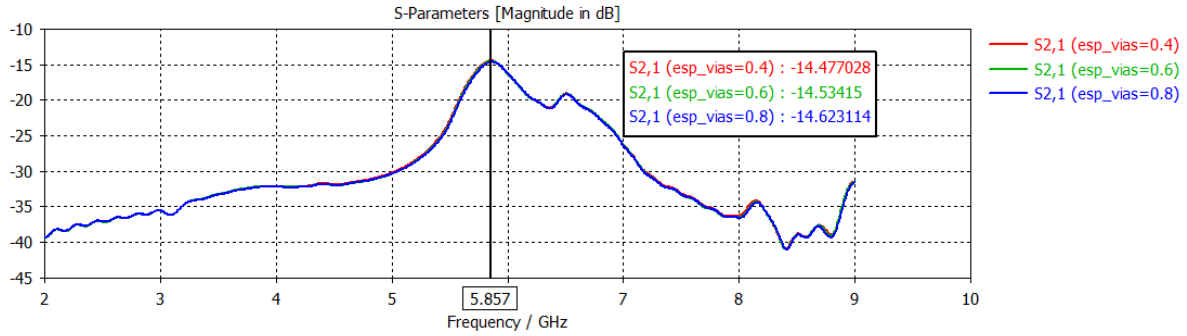

Figure 3.10: Simulated s_{21} of the antenna array of eight elements with the grounded vias

It was clear that the grounded slots would not make a big difference when it comes to mutual coupling decreasing. So it was decided to implement a complementary structure which is presented in the next section.

3.3 Grounded copper vertical plane structure in an 8-element antenna array

In order to explain the problem of mutual effect between structures and how it can be solved by the implementation of a 3D structure, another technique was applied. In Figure 3.11, it is presented how the radiation behaves and, for sure, the increasing of its impact when considering a reduction of space between elements.

Through an overall analysis, an array may benefit from the reflection effect of the metal boundary, so that the current flowing on one element cannot disturb the adjacent ones anymore.

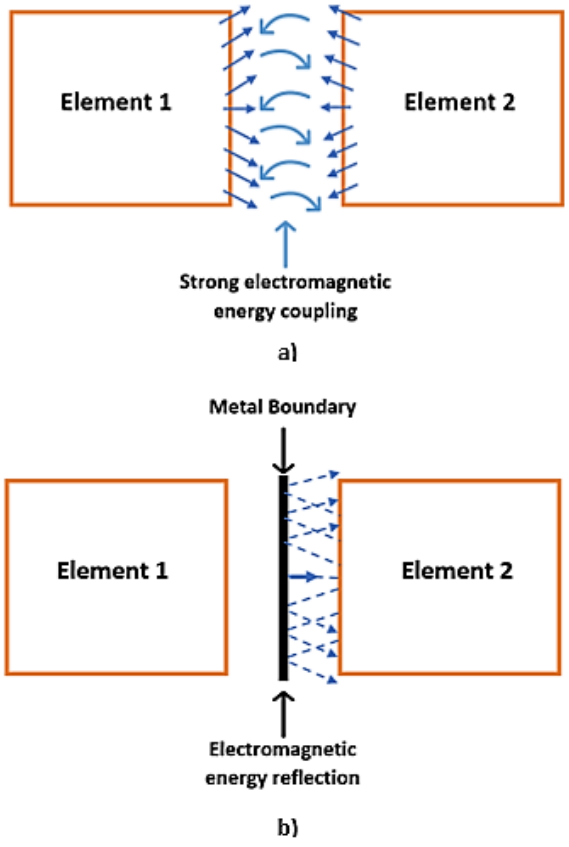

Figure 3.11: Investigation model of mutual effect (a) Strong coupling without metal boundary. (b) Reflection effect of metal boundary.

A schematic of the new implemented technique is shown in Figure 3.12, where periodical cylindrical slots were also added, considering the edge to edge distance between antennas

of 0.1λ, from the top to the ground plane and also a decoupling structure (copper vertical plane) that is placed on the top of the substrate between the patches. The dimensions of the decoupling structure are shown in Table 3.2 and Figure 3.13.

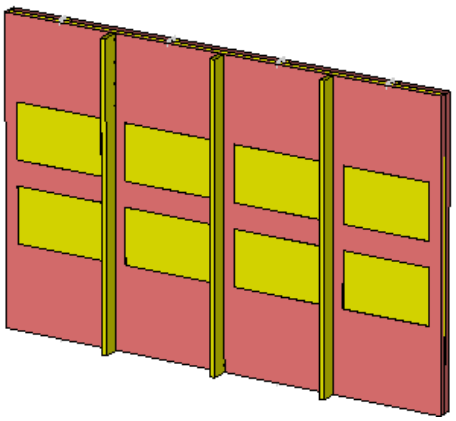

Figure 3.12: Top layer of the 8-element antenna array with the decoupling unit

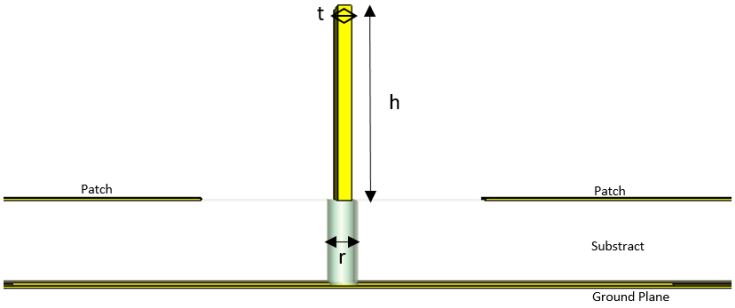

Figure 3.13: Details of slotted ground and copper plane

Symbol	Description	Length (mm)
h	Height of the copper structure	2.1
r	Slot radius	0.4
t	Thickness of the copper structure	1

Table 3.2: 8-element antenna array with decoupling structure parameters

3.3.1 Simulation Results

The S-parameters of the antenna array, after adding the decoupling structure, are shown in Figures 3.14 and 3.15.

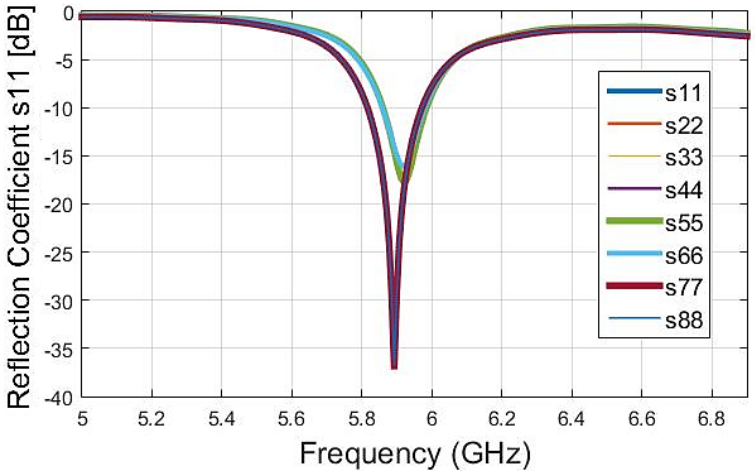

Figure 3.14: Simulated reflection coefficient of the antenna array of eight elements with the decoupling structure

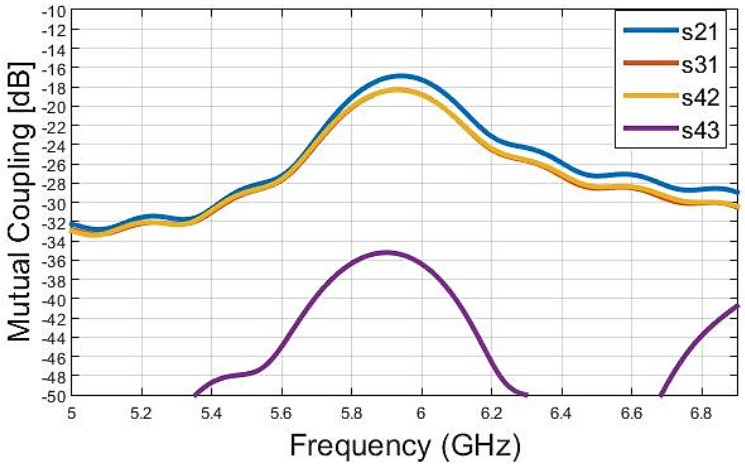

Figure 3.15: Simulated coefficients related to mutual coupling of the antenna array of eight elements with the decoupling structure

With the new structure, the mutual coupling presents a decrease of approximately 3dB when compared to the conventional antenna array, where the reflection coefficient is below -10dB.

3.3.2 Measurement Results

In Figure 3.16 is a photography of the 3D printed board of the antenna array implemented with the decoupling structure.

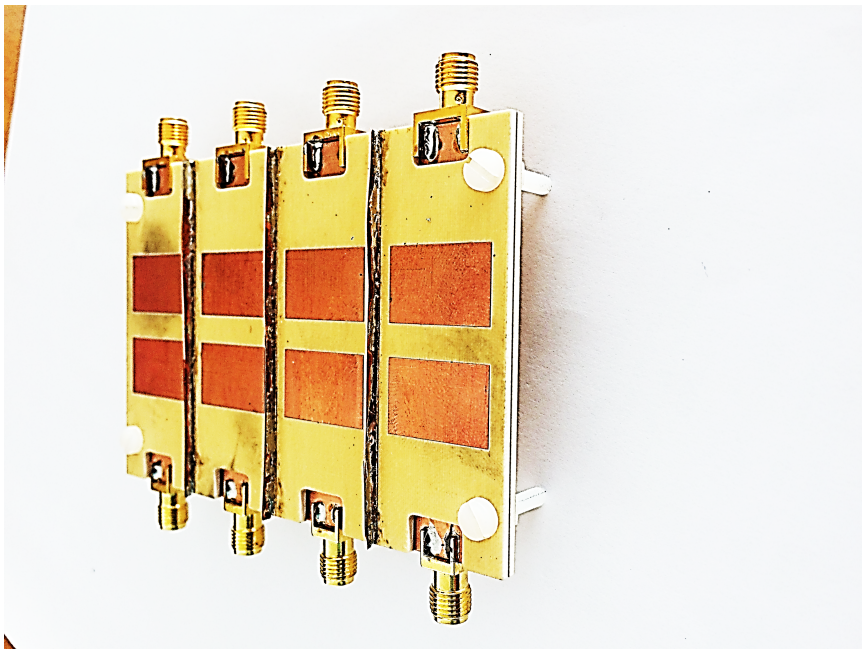

Figure 3.16: Board of the antenna array of eight elements with the decoupling structure

Such as it was presented in the simulation results, the mutual coupling is reduced with the implementation of the vertical plane structure. For a reflection coefficient below -10dB, it was achieved a reduction of 3dB, Figure 3.17 and 3.18.

The expected results were accomplished due to the new implemented copper vertical plane structure, which is responsible for a good suppression of reflections occurred between each patch and, therefore, a decrease of the coupling.

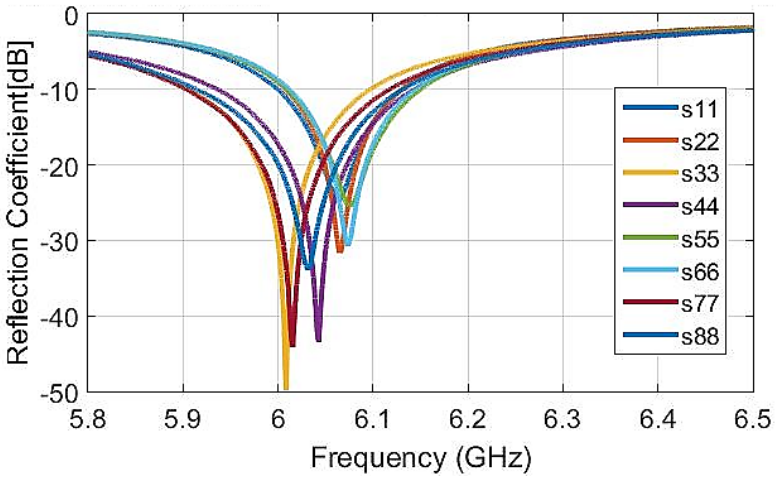

Figure 3.17: Measured reflection coefficient of the antenna array of eight elements with the decoupling structure

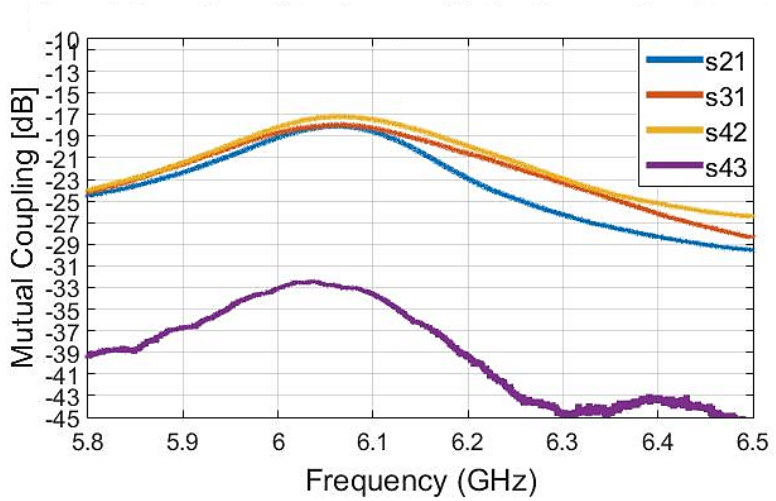

Figure 3.18: Measured coefficients related to mutual coupling of the antenna array of eight elements with the decoupling structure

Chapter 4

Antenna arrays for SATCOM applications

4.1 Series feed Antenna arrays

An analysis of a series feed approach for a N-element microstrip patch antenna array is presented. This chosen approach was designed to achieve optimum omnidirectional beam characteristics and to exhibit pattern stability over frequency in a particular band. The advantages found in using this array topology were the reduction of the distance between elements in an array to have the maximum gain and the less significant side lobes when it comes to the radiation pattern.

Some of the issues inherent to this type of arrays were carefully studied because it was essential to prepare the series feed array to transmit and receive. The ideal array was the one that only had one resonant frequency correspondent to the desired one, to prevent any interference while receiving.

4.1.1 4-element antenna array

It is presented a 4x1 antenna array for a SAR application at 5.3 GHz. A detailed image of the antenna array design and its dimensions are shown in Figure 4.1 and Table 4.1. The array consists of four microstrip patch antennas with line feed located placed on a 0.787-mm-thick Arlon 217Lx substrate (relative permittivity equals 2.17-2.2 at 5.3GHz). The ground plane and the radiating patches are made from copper with 0.035mm.

A. Simulation Results

The adjustments made on the length of the patches($L1$ and $L2$) are an attempt of eliminating the other frequencies for which the array is adapted for. Commonly, this is not a concern in antenna array design. However, this array was conceived to transmit and receive. The other frequencies where the array is adapted are not a concern for transmission. However, once the satellites are in the atmosphere, they receive from multiple equipments radiation values that will cause problems such as noise at the time of the reception.

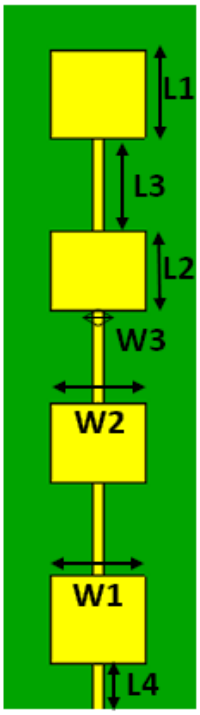

Figure 4.1: Series feed 4-element antenna array

The optimized series feed antenna array presents a reflection coefficient below -10dB for 5.3GHz, Figure 4.2.

Again, it is important to take into account that the impedance on the line feed is as close as possible to the $50 + 0j$, Figures 4.3 and 4.4.

Symbol	Description	Length (mm)
L1	Length of the edge patches	19.4744
L2	Length of the center patches	17.0966
L3	Length of the connection line	20.6897
L4	Length of the feed line	10.3449
W1	Width of the edge patches	20.0658
W2	Width of the center patches	20.9991
W3	Width of the feed line	2.4249

Table 4.1: 4-element series feed antenna array parameters

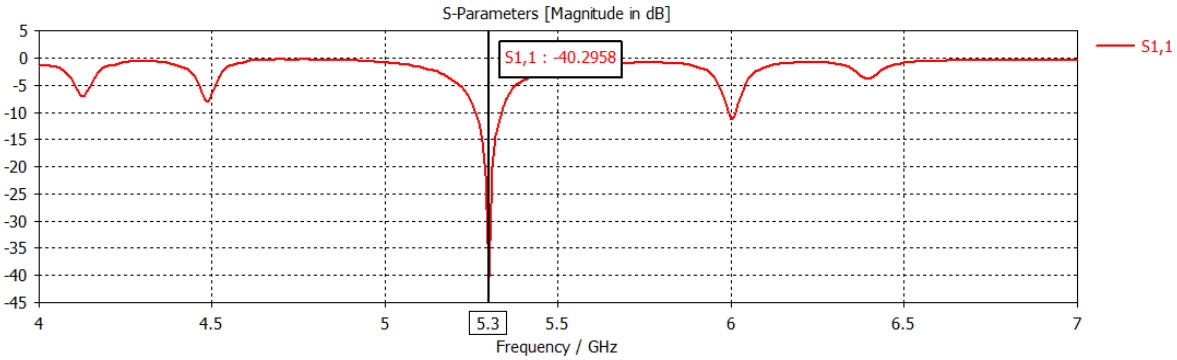

Figure 4.2: Simulated reflection coefficient of a 4-element series feed antenna array

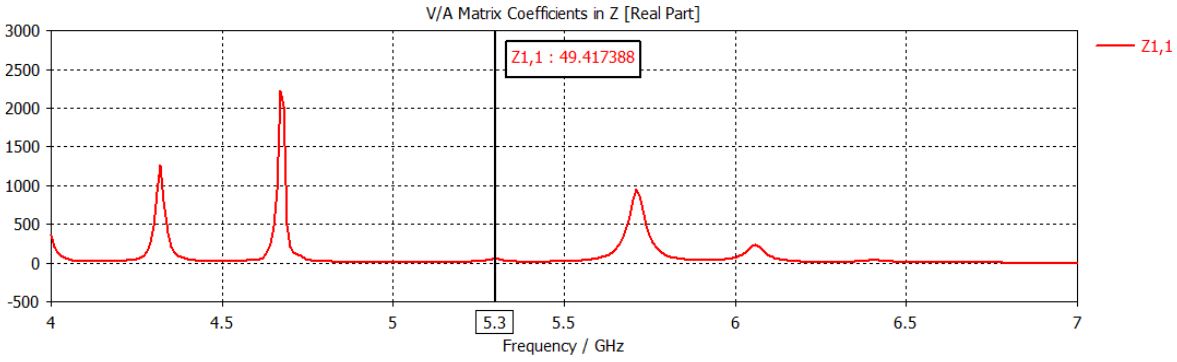

Figure 4.3: Impedance real part

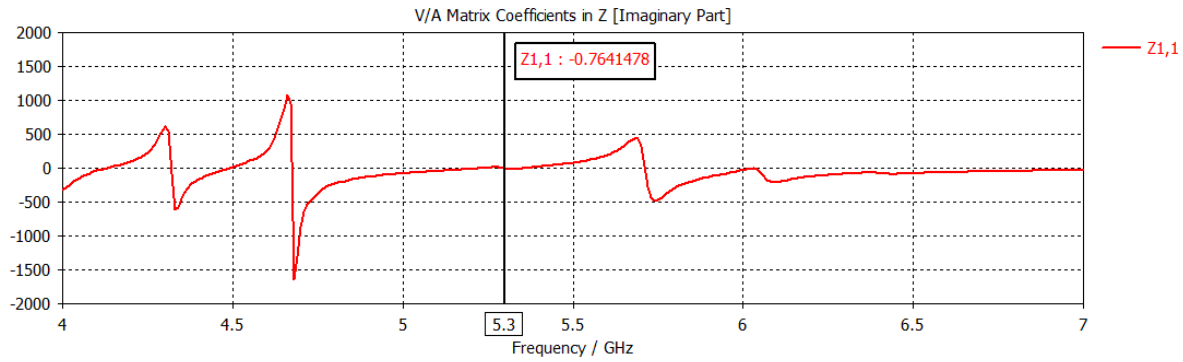

Figure 4.4: Impedance imaginary part

In Figure 4.5, it is visible the limitation that series feed antenna arrays present. Although the problem about the shift could not be solved entirely, there is only a shift phase of 6 degrees, Figures 4.5 and 4.6.

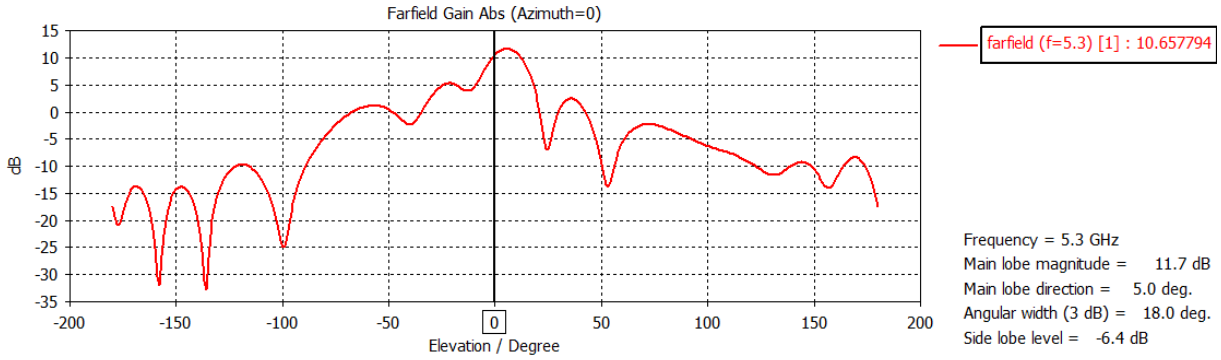

Figure 4.5: 4-element cartesian radiation pattern

If is it considered the theoretical realized gain expected for a patch, between 5 and 6 dB, this array would be expected to have four times more realized gain, which is +6 dB. It is presented a very satisfying value for the array realized gain.

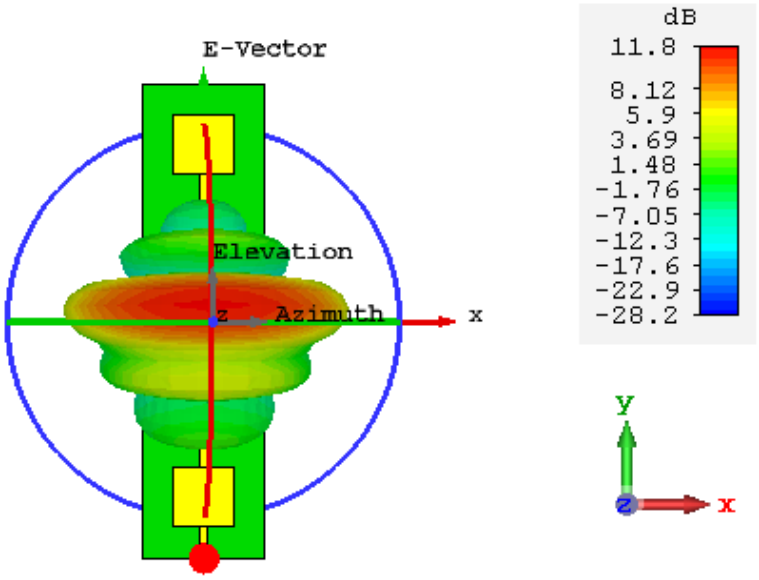

Figure 4.6: 4-element 3D radiation pattern

The radiation pattern of the antenna array illustrates the distribution of radiated power in space. It may be plotted in a spherical coordinate system as the radiated power versus the elevation angle or the azimuth angle. The main lobe that is presented in red, Figure 4.6, has the significant quantity of radiated power. The series feed antenna arrays during this work will have its radiation patterns plotted as the radiated power versus the azimuth angle.

It is evident that in this presented case the biggest challenge is not only the gain achievement but also getting the main lobe direction as close to 0 degrees possible.

B. Measurement Results

The reflection coefficient has a value of -29.14 dB for 5.297 GHz which reveals a very good adaptation of the matching line, Figure 4.7. This is also confirmed in the Smith chart because for the same value of frequency, the value of the z impedance happens to be 50.2576+j3.4942Ω, Figure 4.8.

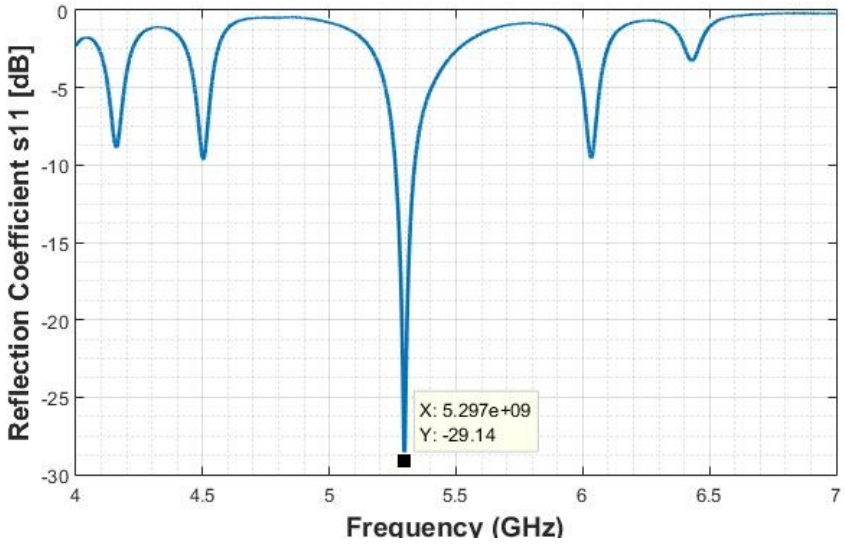

Figure 4.7: Measured reflection coefficient of a 4-element series feed antenna array

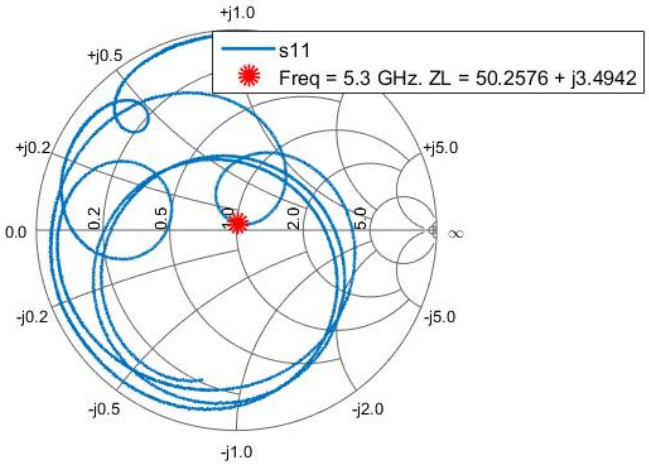

Figure 4.8: Measured Smith Chart

In Figure 4.9, the measured radiation pattern is presented. The expected shift for the phase is 5 degrees. The values for the side lobe levels are under 5 dB which is expected but can be improved. One of the lobes, left lobe, is higher than the right one because of the feed line influence. To reduce this lobe it is possible to add a stub on the other end of the array, but it means more space. The possibility to solve this problem is to change the widths of the patches to reduce the phase shift of 5 dB.

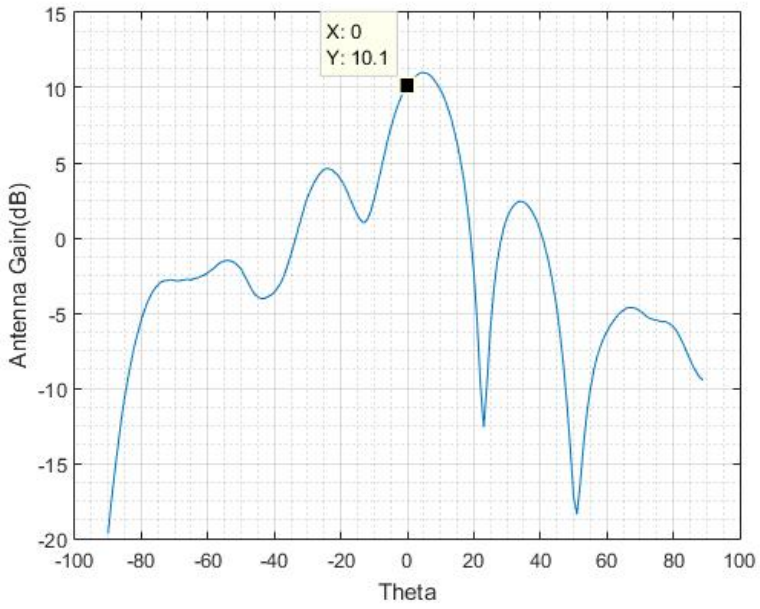

Figure 4.9: Measured radiation pattern

4.1.2 16-element antenna array

The 16-element antenna array uses the same substrate as the 4-element one. It is intended to have four times the number of antennas, and this theoretically causes an increase of 6 dB of realized gain. The distance between the sub-arrays of 4 elements are $\lambda/2$, and the proposed alteration for the width of the edge antennas is implemented. Small alterations were also made in almost all the parameters because the width alterations caused a mismatch for the previous values. The parameter alterations are shown in Figure 4.10 and Table 4.2.

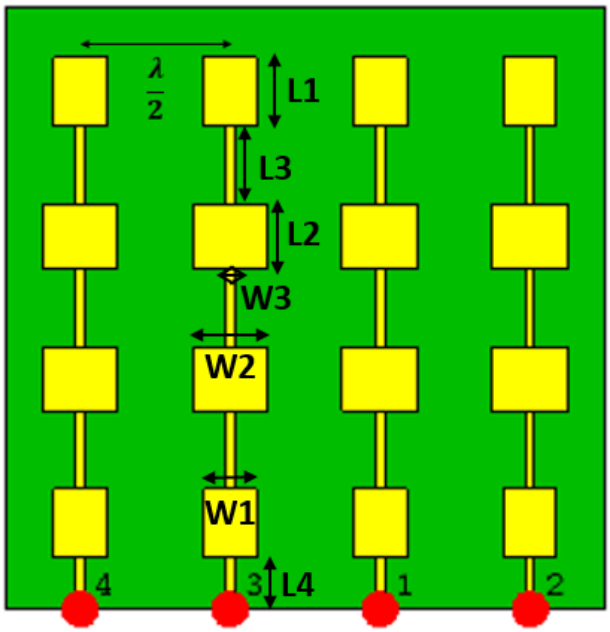

Figure 4.10: Series feed 16-element antenna array

Symbol	Description	Length (mm)
L1	Length of the edge patches	19.1744
L2	Length of the center patches	17.0966
L3	Length of the connection line	21.6897
L4	Length of the feed line	15.3449
W1	Width of the edge patches	14.9158
W2	Width of the center patches	20.9991
W3	Width of the feed line	2.4249

Table 4.2: 16-element series feed antenna array parameters

A. Simulation Results

The result of the reflection coefficient for a single sub-array is presented in Figure 4.11.

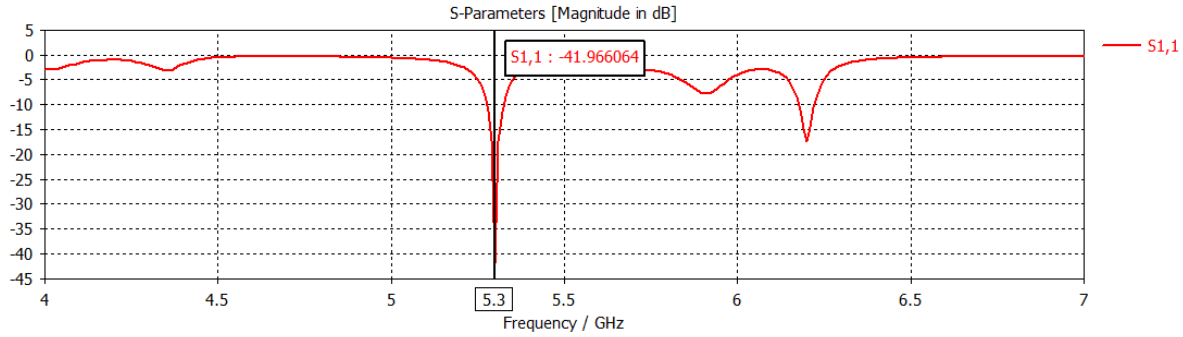

Figure 4.11: Simulated reflection coefficient of a sub-array in the 16-element series feed antenna array

In order to be certain that the results would be just as good for the printed array, it is important to take into account that the impedance on the line feed is as close as possible to the $50 + 0j$, Figures 4.12 and 4.13.

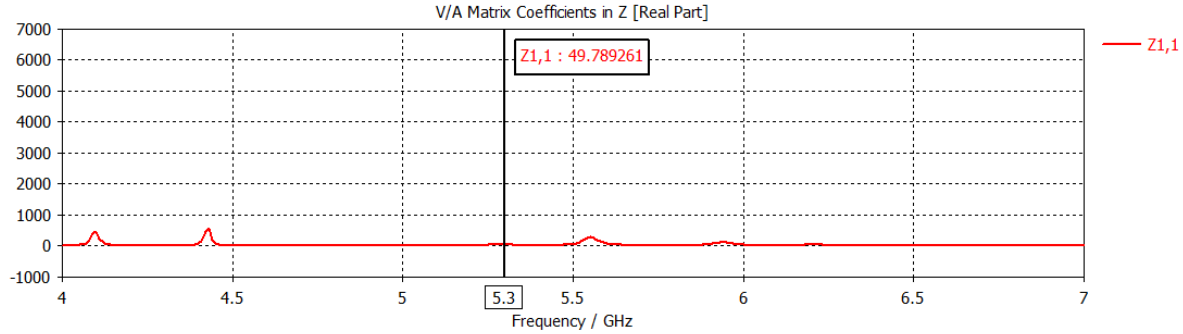

Figure 4.12: Impedance real part

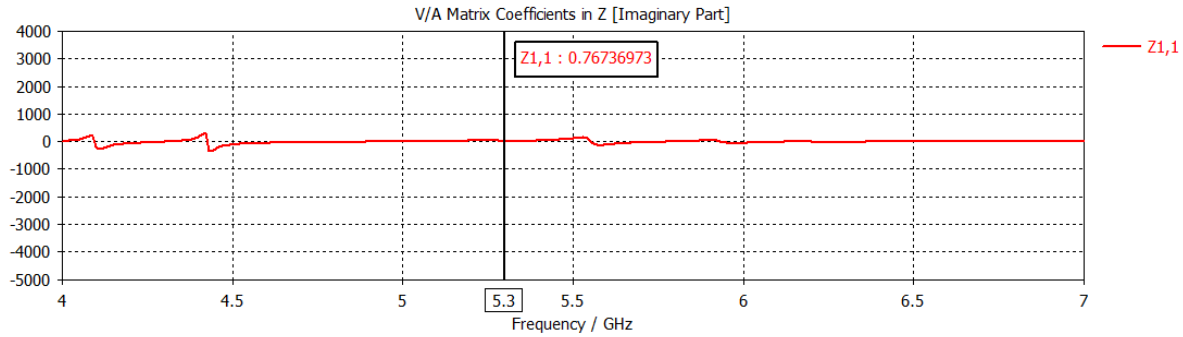

Figure 4.13: Impedance imaginary part

In Figure 4.14, it is visible the limitation that series feed arrays presents, which was previously described. Although the problem about the shift could not be solved entirely,

there is only a shift phase of 4 degrees, Figures 4.14 and 4.15. These 4 degrees will have a minor impact with the increasing number of sub-arrays. Although, a very important issue that is clearly solved is the reduction of the side lobe levels. While in the first approach the side lobe level was -6.4 dB, with the alterations made there is only -13 dB.

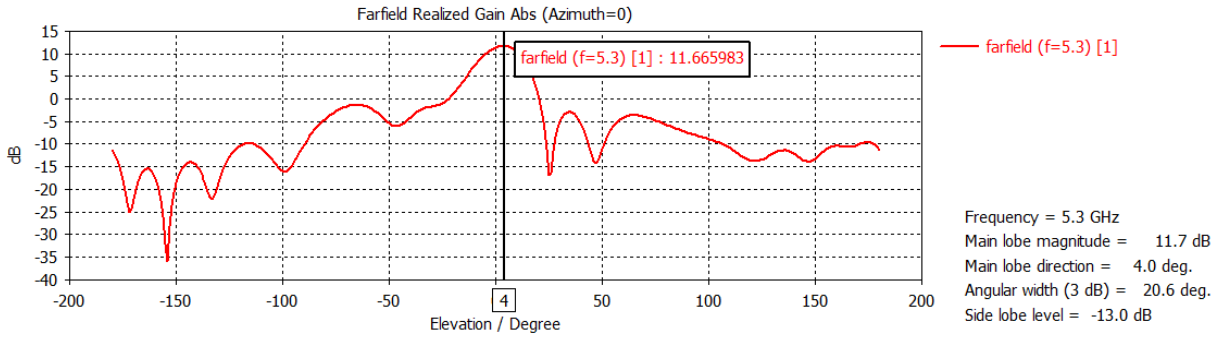

Figure 4.14: 4-element cartesian radiation pattern optimized

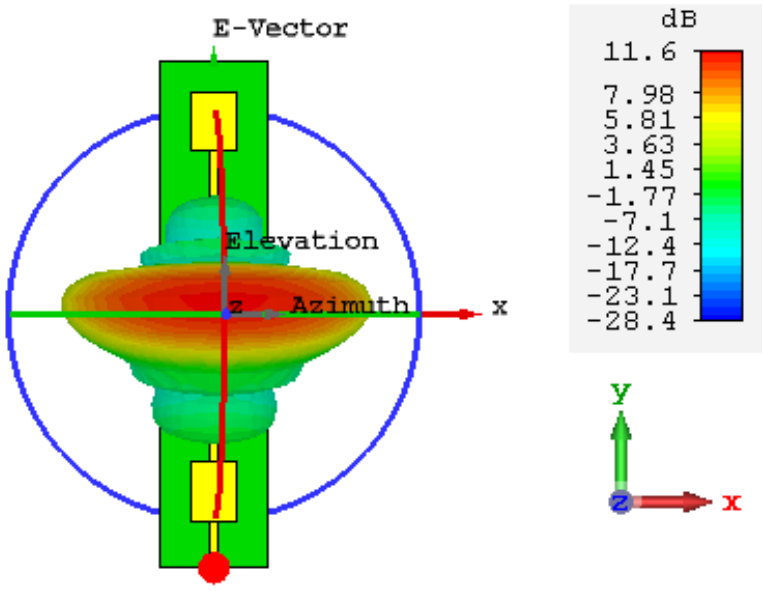

Figure 4.15: 4-element 3D radiation pattern optimized

The simulation results for the 16-element array in a simultaneous simulation are also presented. In Figure 4.16 is shown the results of the reflection coefficient from which is possible to conclude that the adaptation was obtained. To confirm the matching of the feeding line near to the ideal 50 Ω, in Figure 4.17 and 4.18, the values of all the four port impedances are presented.

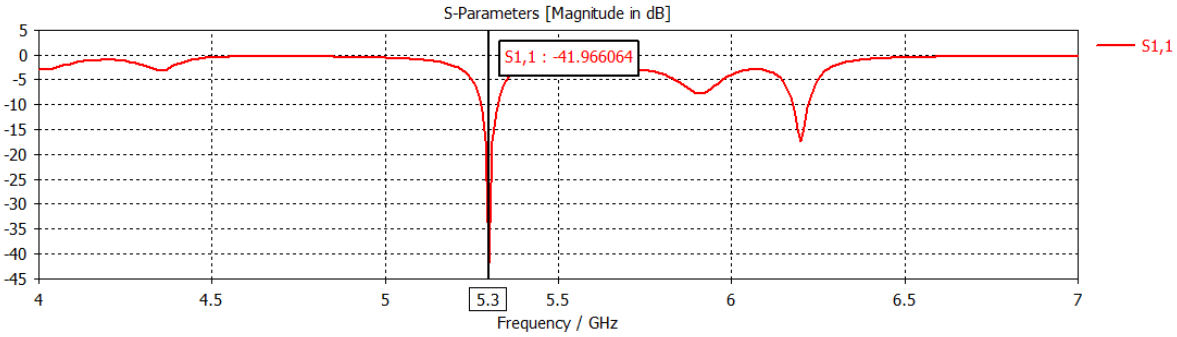

Figure 4.16: Simulated reflection coefficient of a 16-element series feed antenna array

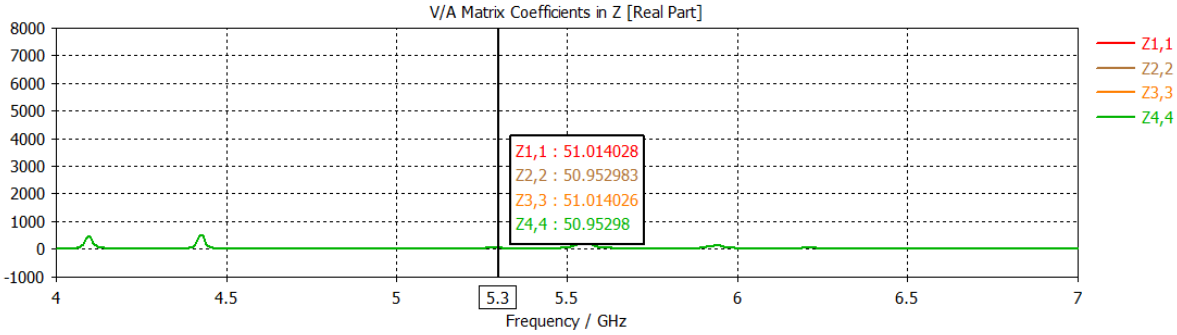

Figure 4.17: Impedance real part

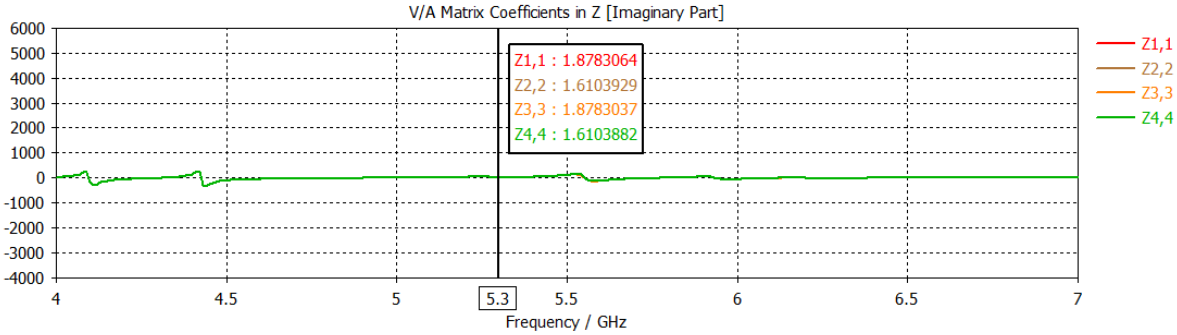

Figure 4.18: Impedance imaginary part

The expected radiation pattern is presented in Figure 4.19 and 4.20. The phase shift of the radiation pattern was reduced to 3 degrees without compromising the reflection coefficient. There is only another frequency that may be filtered where the array is also adapted. As this array is going to be used in both transmission and reception, it is very important to get the phase shift as close as possible to 0 degrees without having too many other frequencies where it is adapted due to the interference of other radiations.

The side lobe level was reduced as it was expected due to the change in the edge patch antennas width.

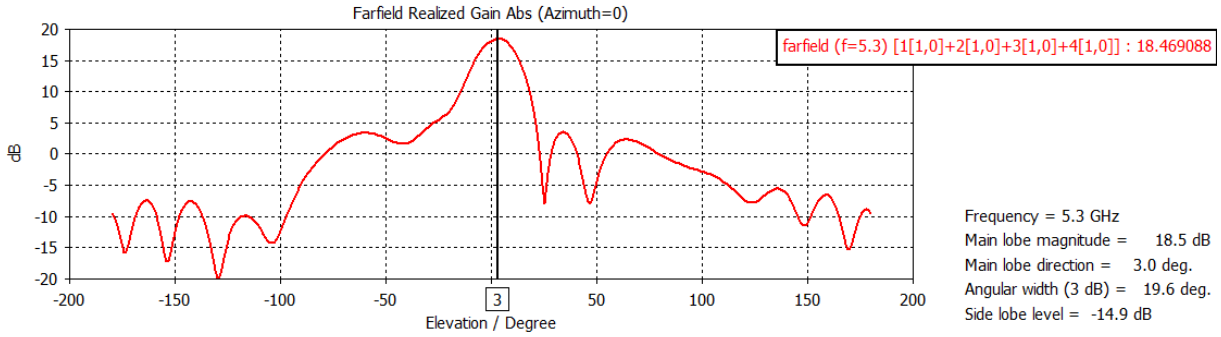

Figure 4.19: 16-element cartesian radiation pattern

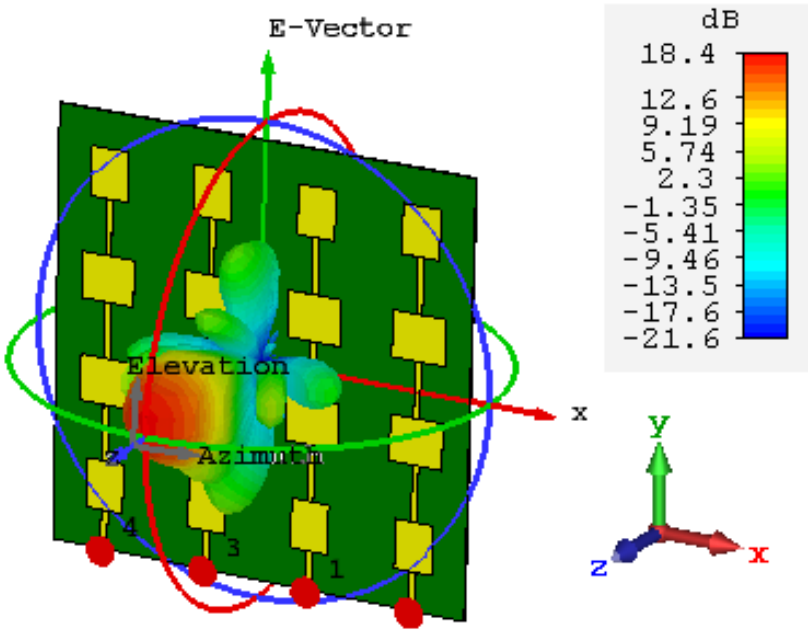

Figure 4.20: 16-element 3D radiation pattern

B. Measurement Results

The array designed was thought to be able to be implemented in a system where it is possible to transmit and receive. This will only be possible by adding a Low Noise Amplifier (LNA) and a Power Amplifier (PA) at the edges of the array. Due to this situation, it can

be concluded that the measured results should approximately match the real system where the array is going to be used.

It was measured the influence of mutual coupling between each sub-array, Figure 4.21. The mutual coupling is way under the -20 dB maximum we look for to consider that there is no interference between each element.

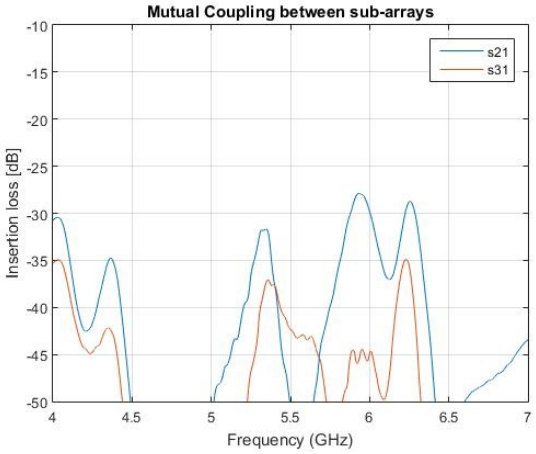

Figure 4.21: Mutual coupling between sub-array 1 and sub-array 2 and 3

In order to get the best results it was used a power splitter ZN4PD1-63+ and SMA cables, Figure 4.22 and 4.23. The total losses are due to the 0.8 dB insertion loss by the power splitter ZN4PD1-63+ and the SMA cables losses of 2.4 dB.

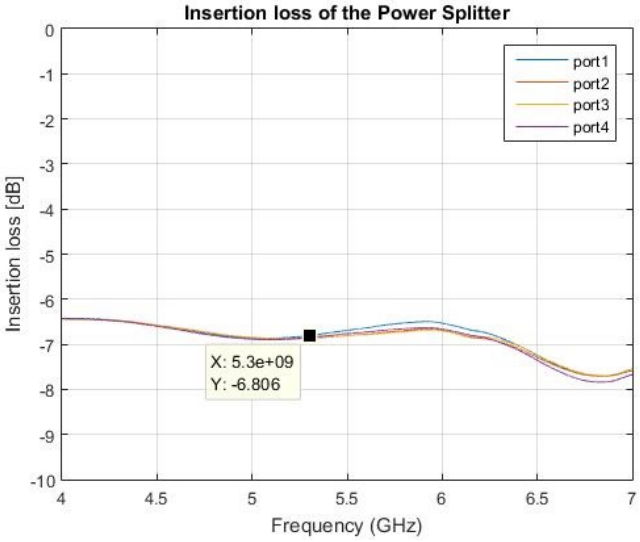

Figure 4.22: Insertion Loss of power splitter

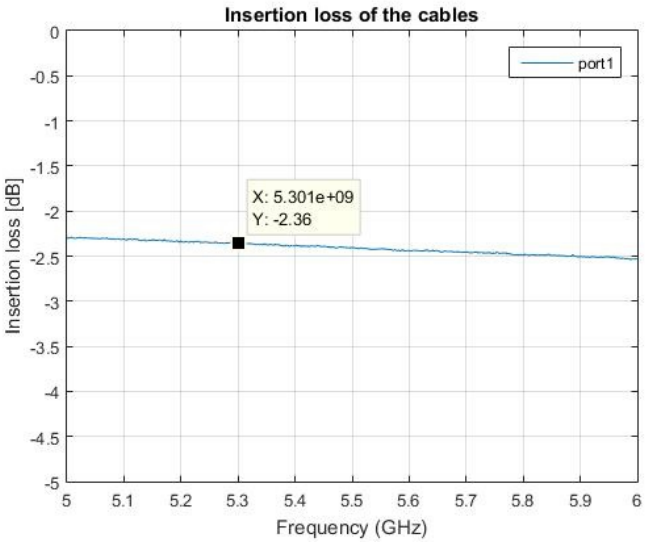

Figure 4.23: Insertion Loss of the SMA cables

The realized gain of the overall array is going to be affected by the previously presented losses. The radiation pattern has still the desired behavior, and there is a reduction of the phase shift for 2 degrees, but above all, there is an almost insignificant value for the side lobe levels. The beam directivity is guaranteed with this configuration.

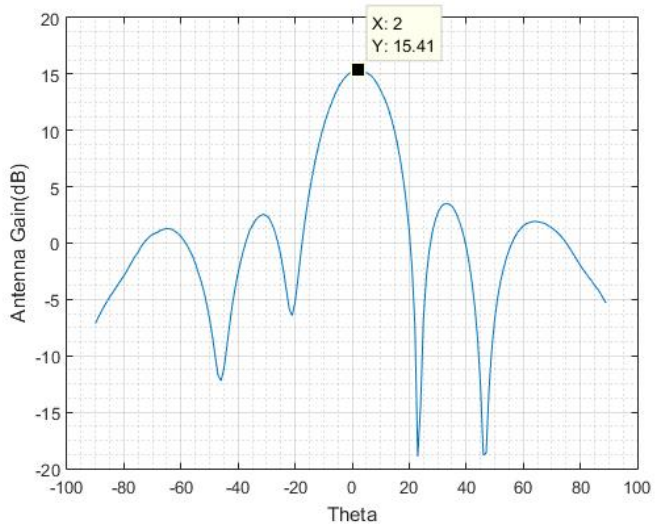

Figure 4.24: Measured radiation pattern of 16-element array

4.2 Circular Polarization patch Antennas

The primary objective of this section is to design an antenna capable of transmitting and receiving with two different feeding lines. To get better isolation between the radiating element and the feed lines, the chosen feed technique was the aperture coupled feed.

4.2.1 Blended edges Technique

It is presented a microstrip patch antenna with circular polarization for a SAR application at 5.3 GHz. Circular polarized antennas are very common in SAR application because there is a possibility of transmitting and receiving in two different polarization.

A detailed image of the antenna array design and its dimensions are shown in Figures 4.25 and 4.26. The antenna consists of a rectangular aperture coupled feed with a slot located in the ground plane, placed on a 0.787-mm-thick Arlon 217Lx substrate (relative permittivity equals 2.17-2.2 at 5.3GHz). The ground plane and the radiating patches are made from copper with 0.035mm of thickness, and the slot of each element is excited by a 50Ω microstrip located on the back of the bottom layer. The value of width and length of the antenna must be equal in order to get circular polarization.

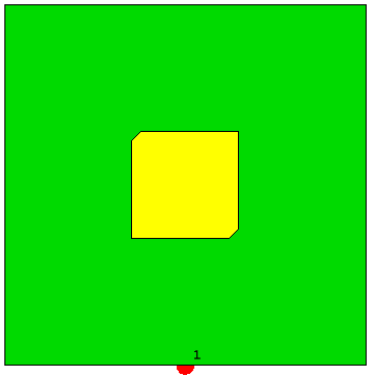

Figure 4.25: Patch antenna with circular polarization front view

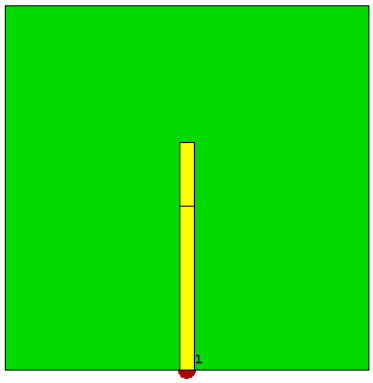

Figure 4.26: Patch antenna with circular polarization back view

In Figure 4.27, 4.28 and 4.29 is presented the reflection coefficient and the feed line impedance, respectively.

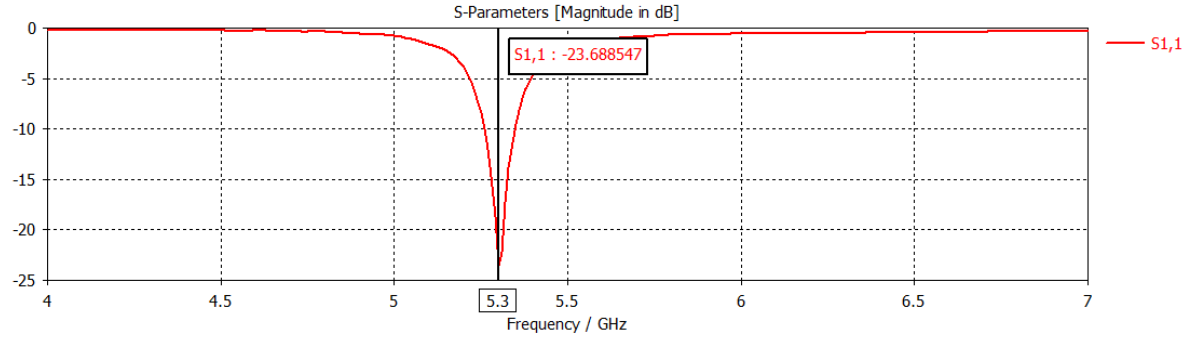

Figure 4.27: Reflection coefficient of the patch antenna with circular polarization front view

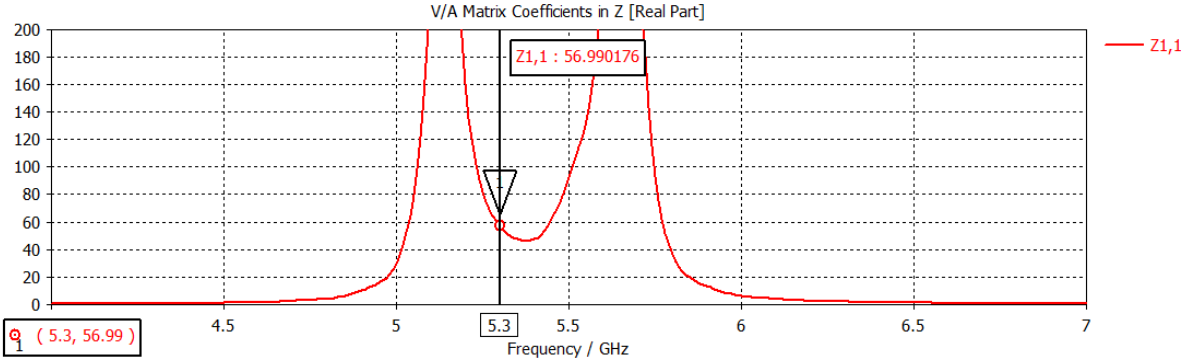

Figure 4.28: Impedance real part

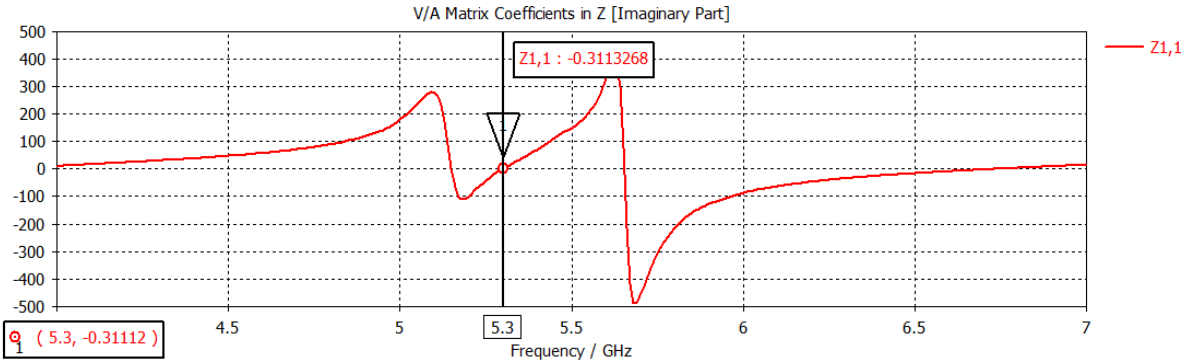

Figure 4.29: Impedance imaginary part

The matching for 5.3 GHz was satisfying. However, in this case, we look for an antenna with circular polarization. Previously, it was discussed that to have a circular polarization in an antenna the value for the AR should be as near as possible to 0 dB. The value obtained is presented in Figure 4.30 and for 5.3GHz it is approximately 0.41 dB.

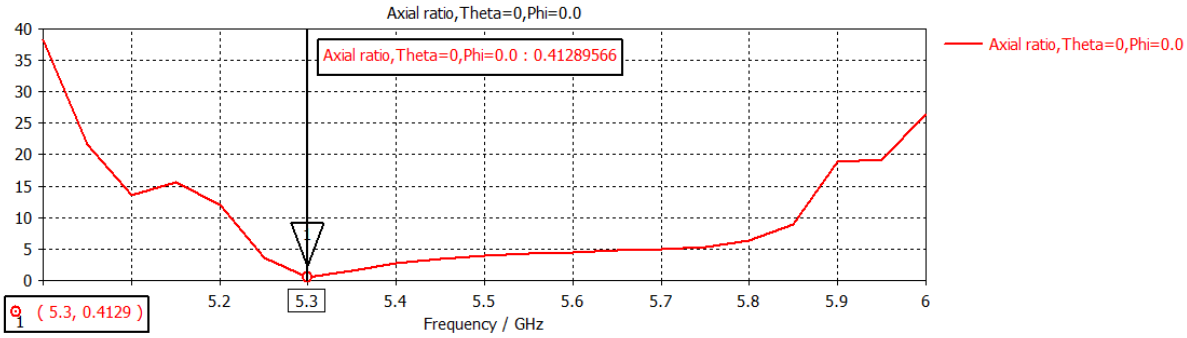

Figure 4.30: Axial Ratio

4.2.2 Two feed Circular Polarization Patch Antenna

In the previous section, we could conclude that it is possible to get an antenna using aperture feed with circular polarization. The next step is to try to get the same results using two transmitting lines. The front plane is presented in Figure **??** while the back plane where the feed lines are placed is presented in Figure 4.32.

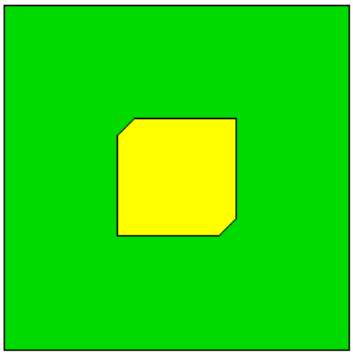

Figure 4.31: Patch antenna with two feed lines front view

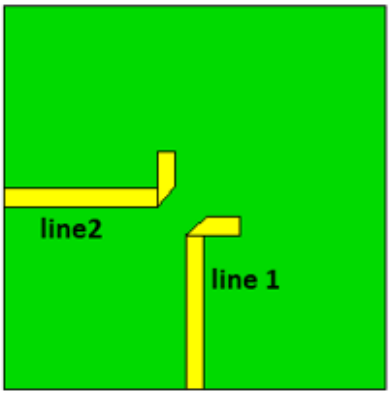

Figure 4.32: Patch antenna with two feed lines back view

The biggest disadvantage of this implementation is that when the axial ratio starts to decrease, Figure 4.33, the mutual coupling between ports 1 and 2, that are related to lines 1 and 2, starts increasing, Figure 4.34.

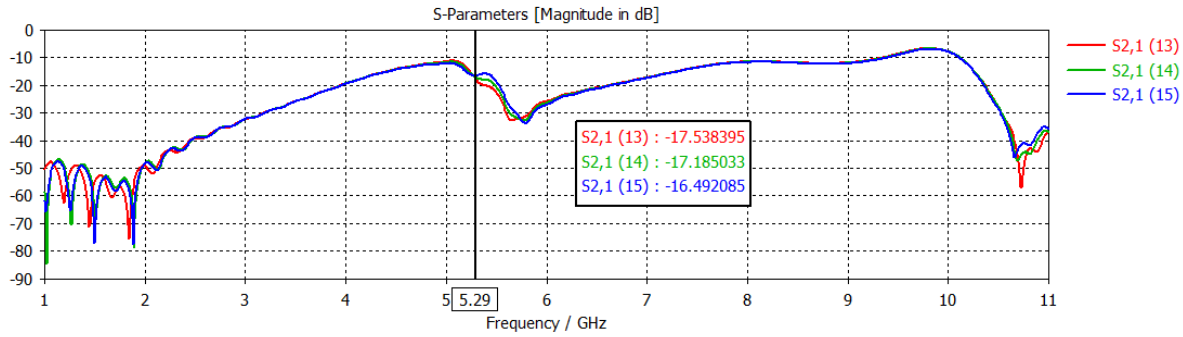

Figure 4.33: Mutual coupling between port 1 and port 2 of the patch antenna with two feed lines

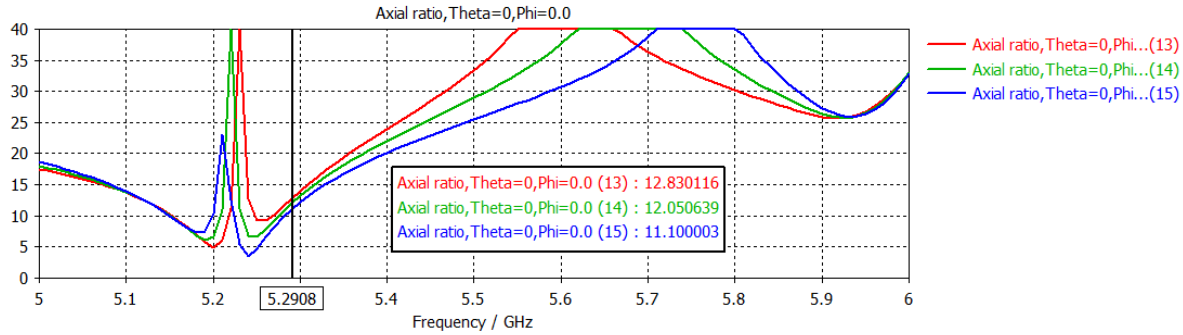

Figure 4.34: Axial Ratio of the patch antenna with two feed lines

The advantage of trying this technique is the less complexity it would bring to an antenna array design. The results were not satisfying, so the last step was to implement a quadrature hybrid coupler to get the circular polarization.

4.2.3 Circular Polarization Patch Antenna with a quadrature hybrid coupler

To have circular polarization, a quadrature hybrid coupler was designed, Figure 4.35.

A. Quadrature hybrid coupler design

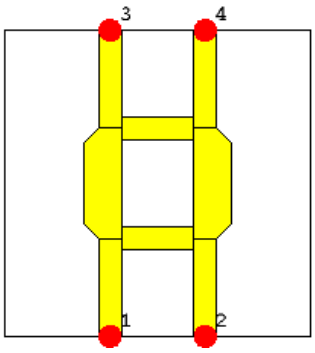

Figure 4.35: Quadrature hybrid coupler schematic

The construction of a quadrature hybrid coupler is made with quarter-wavelength sections of transmission lines, Figure 4.36. They are a special case of directional couplers, where the coupling factor is 3 dB. The quadrature hybrid has a 90° phase shift between ports 2 and 3, while fedding at port 1.

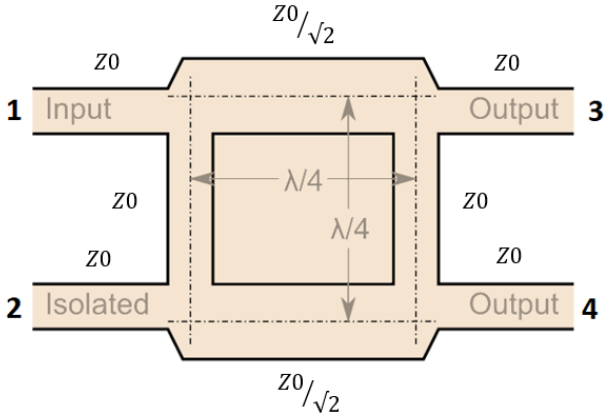

Figure 4.36: Quadrature hybrid coupler design

In Figure 4.37, it is shown the reflection coefficient for a 5.3GHz quadrature hybrid coupler. In Figure 4.38, it is presented the isolation between port 1 and port 2 and in Figure 4.39, the phase shift of 90° between port 3 and port 4 is presented.

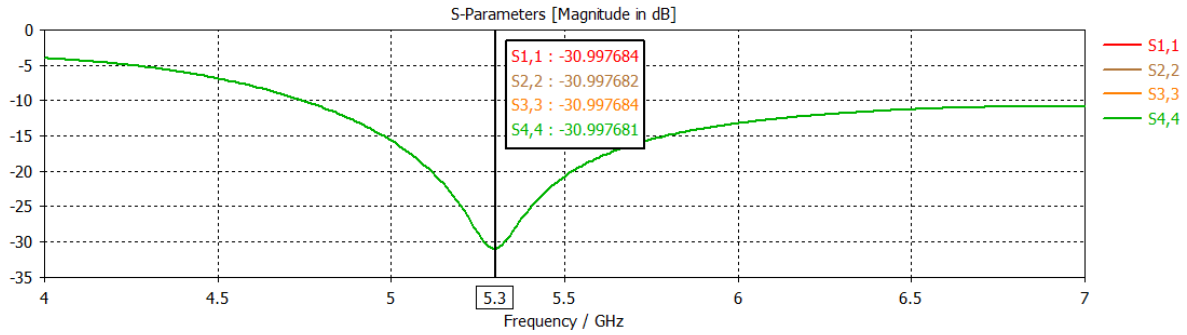

Figure 4.37: Reflection coefficient of quadrature hybrid coupler ports

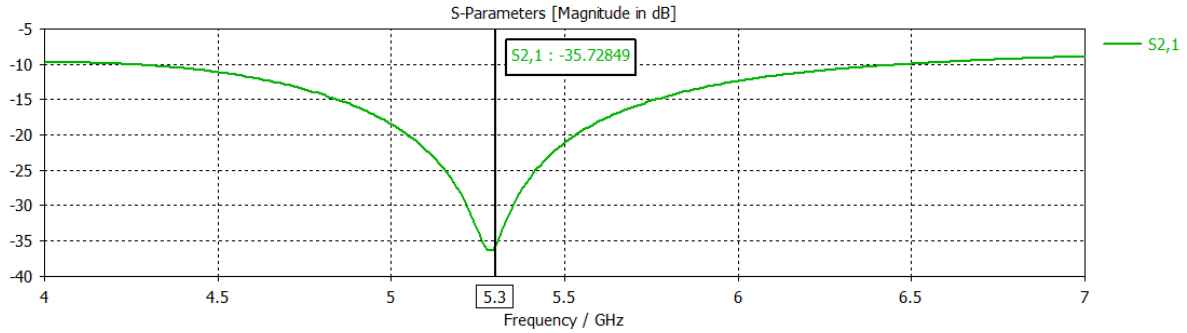

Figure 4.38: Isolation between port 1 and port 2

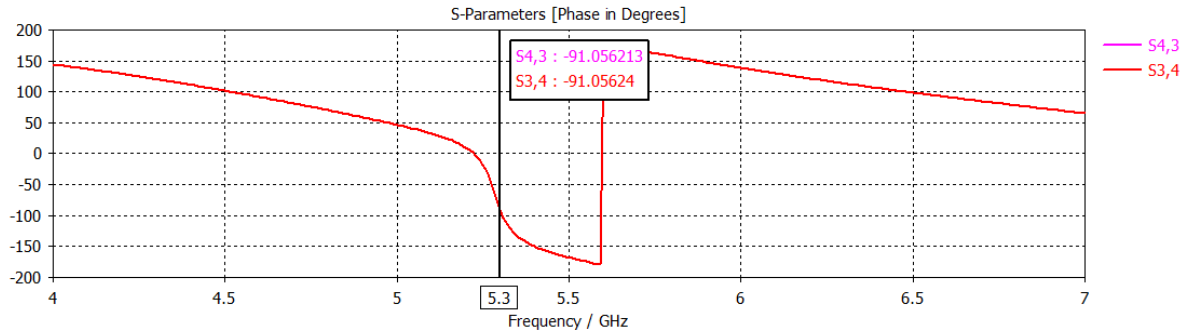

Figure 4.39: Phase shift between port 3 and port 4

The coupling factor should theoretically be 3 dB, but the values were slightly different, Figure 4.40. The maximum deviation from the 3 dB was for 0.54 dB that is irrelevant for the final results.

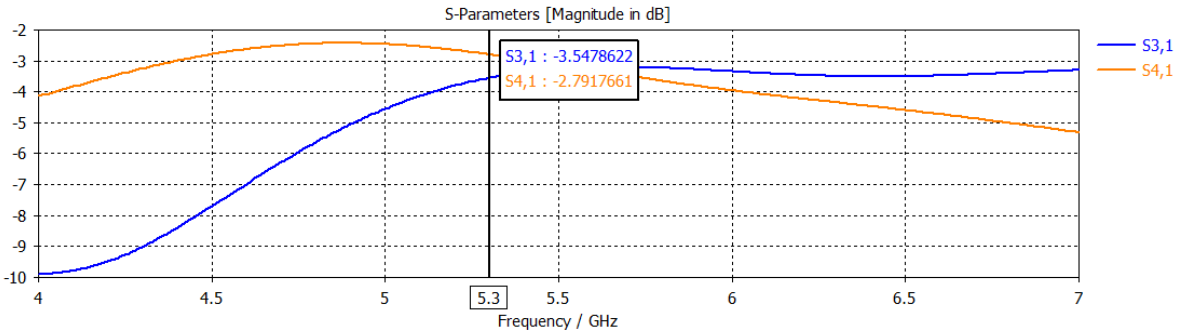

Figure 4.40: Coupling factor between port 1 and port 3 and 4

B. Patch antenna with quadrature hybrid coupler feed

Using a quadrature hybrid coupler, Figure 4.42, as a feed line to the microstrip patch antenna, it will be possible to have the circular polarization once the hybrid itself adds between port 1 and port 2, Figure 4.41, a phase shift of 90° and has the isolation between port 1 and port 2 desired.

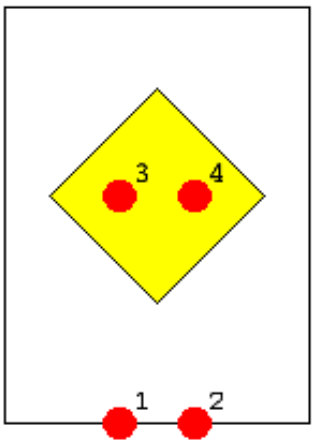

Figure 4.41: Patch antenna with a quadrature hybrid coupler front view

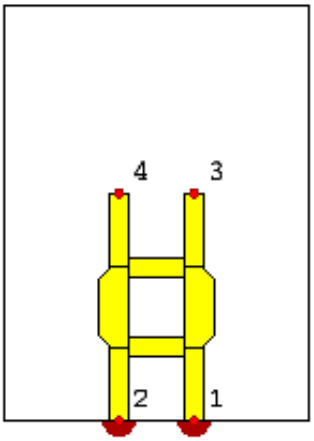

Figure 4.42: Patch antenna with a quadrature hybrid coupler back view

The adaptation of the microstrip patch antenna is pleasant, but it has very high bandwidth. When implemented in an array, the bandwidth narrows, so having high bandwidth at this point is acceptable, Figure 4.43.

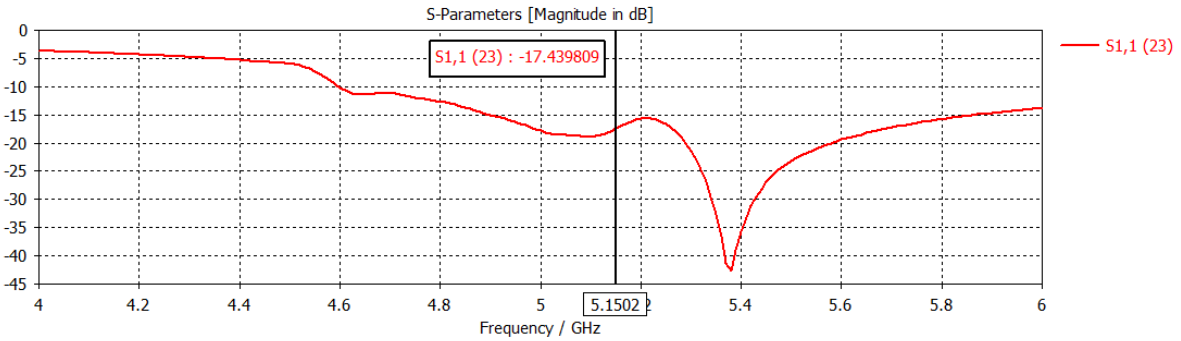

Figure 4.43: Reflection coefficient of the patch antenna with a quadrature hybrid coupler

The rejection pretended between port 1 and port 2 is a very important parameter that is going to define if the circular polarization is going to be a valuable input because it dictates if the antenna is suitable for transmission and reception separately, Figure 4.44. The axial ratio was near 0 dB as expected, Figure 4.45.

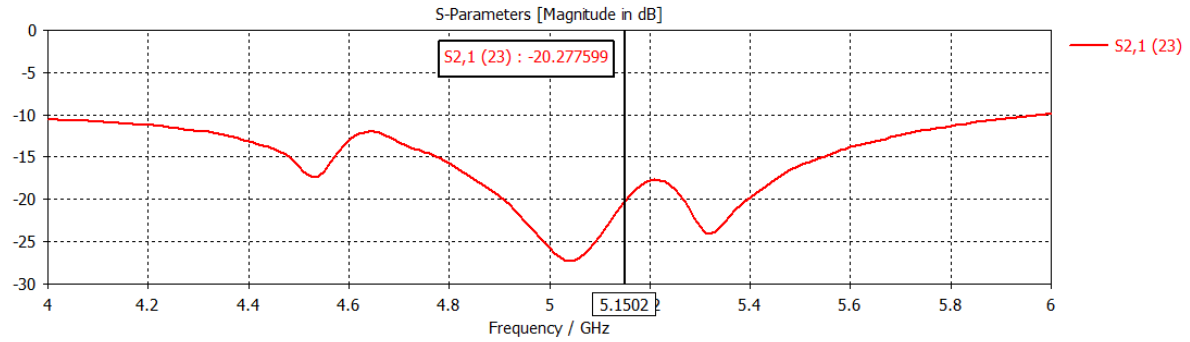

Figure 4.44: s_{21} between port 1 and port 2 of the patch antenna with a quadrature hybrid coupler

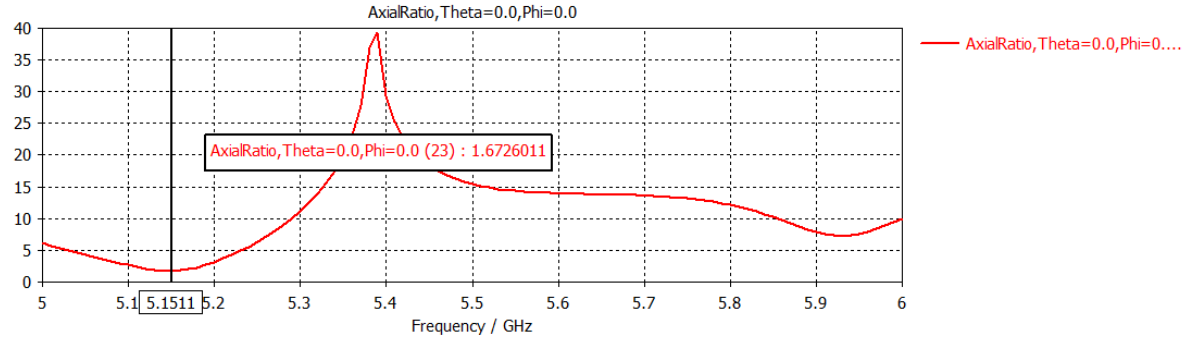

Figure 4.45: Axial Ratio of patch antenna with a quadrature hybrid coupler

Chapter 5

Conclusions and Future Work

5.1 Conclusions

The development of telecommunications systems has been growing regarding antenna arrays limitations. The improvement of antenna arrays and its potential to overcome some of the issues, such as higher data rates or lower latencies, justifies the presented study of alternative methods to reduce mutual coupling.

The implementation of an 8-element antenna array was developed using the aperture coupled feed technique because the intention was to understand the coupling between microstrip patch antennas without considering the feed lines. This kind of feeding technique is the one that has less spurious radiation due to the isolation between each plane. Although the slotted ground plane did not have good results in terms of the mutual coupling decrease, the afterwards proposed grounded vertical structure had a reduction of 3 dB in mutual coupling which corresponds to half of the power in the closest port when the other has been excited.

The series feed patch antenna arrays implemented had very satisfying results with a 4-element antenna array with 10.1 dB of measured realized gain when it would theoretically been between 11 and 12 dB. The 16-element antenna array had 15.7 dB. Nevertheless, there were some limitations in measuring the realized gain of this antenna array because of the losses related to SMA cables and the power splitter.

Finally, the circular polarized microstrip patch antennas had pleasant results relatively to the axial ratio. The first challenge while designing them was to understand if with aperture coupled feed it was possible to achieve circular polarization, and consequently if the hybrid feed was the only way to separate transmission and reception. The best results happened to be at 5.15 GHz. Although the high bandwidth may be a concern, it should

only be taken into account when the overall array has been designed. A specific bandwidth should be accomplished by that time.

5.2 Future Work

Regarding the reduction of mutual coupling, there are limitations in the presented solution because even considering the use of a higher vertical plane, with which it would be possible to reduce even more the mutual coupling, it would be a concern to lose vertical space. An alternative to this would be to make a study with materials other than copper. Another valuable solution is to reshape the vertical copper structure and make it a triangle to reduce the reflection in the copper plane back to the emitting antenna.

The series feed patch antenna arrays may constitute a good solution to make new implementations such as active antenna arrays. Certainly, it is possible to change the main beam direction with only resizing the edge microstrip patch antennas. This conclusion leads to an opportunity of studying those methods and use them for beam controlling in any application.

The antenna arrays for SATCOM should be refined. Some research on how the circular polarization is a valuable input to separate transmission and reception should be performed because the quadrature hybrid coupler occupies more space and adds a new substrate layer.

Bibliography

[1] Noor Hidayah Muhamad Adnan, Islam Md Rafiqul, and AHM Zahirul Alam. "Massive MIMO for Fifth Generation (5G): Opportunities and Challenges". In: *Computer and Communication Engineering (ICCCE), 2016 International Conference on*. IEEE. 2016, pp. 47–52.

[2] Erik Dahlman et al. "5G wireless access: requirements and realization". In: *IEEE Communications Magazine* 52.12 (2014), pp. 42–47.

[3] Elias Yaacoub, Mohammed Husseini, and Hassan Ghaziri. "An overview of research topics and challenges for 5G massive MIMO antennas". In: *Antennas and Propagation (MECAP), 2016 IEEE Middle East Conference on*. IEEE. 2016, pp. 1–4.

[4] A Balanis Constantine et al. *Antenna theory: analysis and design*. 2005.

[5] Yi Huang and Kevin Boyle. *Antennas: from theory to practice*. John Wiley & Sons, 2008.

[6] Houda Werfelli et al. "Design of rectangular microstrip patch antenna". In: *Advanced Technologies for Signal and Image Processing (ATSIP), 2016 2nd International Conference on*. IEEE. 2016, pp. 798–803.

[7] Lal C Godara. "Applications of antenna arrays to mobile communications. I. Performance improvement, feasibility, and system considerations". In: *Proceedings of the IEEE* 85.7 (1997), pp. 1031–1060.

[8] H Carrasco et al. "Mutual coupling between planar inverted-F antennas". In: *Microwave and optical technology letters* 42.3 (2004), pp. 224–227.

[9] Christophe Caloz et al. "A simple and accurate model for microstrip structures with slotted ground plane". In: *IEEE microwave and wireless components letters* 14.3 (2004), pp. 127–129.

[10] G Dadashzadeh et al. "Mutual coupling suppression in closely spaced antennas". In: *IET microwaves, antennas & propagation* 5.1 (2011), pp. 113–125.

[11] H Wang, DG Fang, and P Ge. "Mutual coupling reduction between two conformal microstrip patch antennas". In: *Environmental Electromagnetics, 2009. CEEM 2009. 5th Asia-Pacific Conference on.* IEEE. 2009, pp. 176–179.

[12] Mohamed Elhefnawy and Josaphat Tetuko Sri Sumantyo. "A review on designing antenna arrays for long range synthetic aperture radar". In: *Recent Advances in Robotics and Sensor Technology for Humanitarian Demining and Counter-IEDs (RST), International Workshop on.* IEEE. 2016, pp. 1–5.

[13] Dennis Roddy. *Satellite Communications, (Professional Engineering).* McGraw-Hill Professional: New York, 2006.

[14] Tursunjan Yasin and Reyhan Baktur. "Circularly polarized meshed patch antenna for small satellite application". In: *IEEE Antennas and Wireless Propagation Letters* 12 (2013), pp. 1057–1060.

[15] Xinyu Liu et al. "Transparent and Nontransparent Microstrip Antennas on a CubeSat: Novel low-profile antennas for CubeSats improve mission reliability." In: *IEEE Antennas and Propagation Magazine* 59.2 (2017), pp. 59–68.

[16] Ralph Pokuls, Jaroslaw Uher, and DM Pozar. "Microstrip antennas for SAR applications". In: *IEEE Transactions on Antennas and Propagation* 46.9 (1998), pp. 1289–1296.

[17] Randy Bancroft. *Microstrip and printed antenna design.* The Institution of Engineering and Technology, 2009.

[18] Krzysztof Wincza and Slawomir Gruszczynski. "Microstrip antenna arrays fed by a series-parallel slot-coupled feeding network". In: *IEEE Antennas and Wireless Propagation Letters* 10 (2011), pp. 991–994.

[19] Tao Yuan, Ning Yuan, and Le-Wei Li. "A novel series-fed taper antenna array design". In: *IEEE antennas and wireless propagation letters* 7 (2008), pp. 362–365.

[20] Sohini Sengupta, David R Jackson, and Stuart A Long. "A method for analyzing a linear series-fed rectangular microstrip antenna array". In: *IEEE Transactions on Antennas and Propagation* 63.8 (2015), pp. 3731–3736.

[21] Hiroki Tsutsumi, Yoshihiko Kuwahara, and Hiroyuki Kamo. "Design of the series fed microstrip patch planar array antenna by the parato genetic algorithm". In: *Antennas and Propagation & USNC/URSI National Radio Science Meeting, 2015 IEEE International Symposium on.* IEEE. 2015, pp. 1854–1855.